PERFORMANCE OF DEEP GEOTHERMAL ENERGY SYSTEMS

Dissertation submitted in partial fulfillment for the award of the degree of Master of Applied Sciences

In

Environmental Engineering

By

Nikhil Manikonda

Faculty of Graduate and Postdoctoral Studies

Department of Civil Engineering

University of Ottawa

Ontario, Canada.

ACKNOWLEDGEMENTS

First and foremost, I offer my obeisance to the Almighty for having bestowed his grace. I humbly present this research as a part of my curriculum, which contains the details of research work on the “Performance of deep geothermal energy systems”.

I sincerely wish to acknowledge and thank my supervisor Dr. Majid Mohammadian for his deep sincerity, support, and guidance throughout the research work, whose kind cooperation helped me collect sufficient information for the completion of this work

I am very thankful to all my friends and family members for their support and encouragement during the dissertation. Most importantly, I thank my girlfriend for pushing me forward and reminding me that I was capable of doing it, even when I was down.

Nikhil Manikonda

Abstract

Geothermal energy is an important source of clean and renewable energy. This project deals with the study of deep geothermal power plants for the generation of electricity. The design involves the extraction of heat from the Earth and its conversion into electricity. This is performed by allowing fluid deep into the Earth where it gets heated due to the surrounding rock. The fluid gets vaporized and returns to the surface in a heat pipe. Finally, the energy of the fluid is converted into electricity using turbine or organic rankine cycle (ORC). The main feature of the system is the employment of side channels to increase the amount of thermal energy extracted. A finite difference computer model is developed to solve the heat transport equation. The numerical model was employed to evaluate the performance of the design. The major goal was to optimize the output power as a function of parameters such as thermal diffusivity of the rock, depth of the main well, number and length of lateral channels. The sustainable lifetime of the system for a target output power of 2 MW has been calculated for deep geothermal systems with drilling depths of 8000 and 10000 meters, and a financial analysis has been performed to evaluate the economic feasibility of the system for a practical range of geothermal parameters. Results show promising an outlook for deep geothermal systems for practical applications.

Table of Contents

List of Figures:

List of Tables:

Abbreviations:

BHE: Borehole heat exchanger

EGS- Enhanced geothermal system

FD- Finite difference

FE- Finite element

GCHP- Ground coupled heat pump

GHE- Ground heat exchanger

GHP- Geothermal heat pump

GSHP: Ground source heat pump

HDR- Hot dry rock

ORC- Organic rankine cycle

PDC- Polycrystalline diamond compact

TRCM- Thermal resistance and capacity models

UGCHE- U vertical ground coupled heat exchanger

Symbols:

T = Fluid temperature in the in-pipe

u = refrigerant fluid velocity

ϕ = specific heat transfer co-efficient

z = vertical coordinate

T_s = vertical soil temperature

D = depth

Δt = time step size

T = temperature

$T_{i,j,k}^{n}$ = temperature at time $t = n\Delta t$ at the location represented by the gird point *(i, j,k)*

$T_{i,j,k}^{n+1}$ = temperature at time $t = (n+1)\Delta t$ at the location represented by the gird point *(i, j,k)*

K_x, K_y and K_z = respectively the thermal diffusion coefficient in *x, y,* and *z* directions

t = the time

S = the heat source or sink

$\Delta v = \Delta x \times \Delta y \times \Delta z$ = volume of the computational cell

Overview:

Objectives of the present study

The following objectives are considered in this study:

- To design a geothermal power plant that can generate 2 MW of electricity and follow the given demand curve.
- To estimate system lifetime under various conditions using numerical simulations.
- To obtain the optimal conditions which lead to maximum system life time.
- To conduct a financial analysis in order to make sure that the system is economical.

Methodology

A numerical approach has been employed in this project to design an economical geothermal power plant system. Initially, an imaginary geothermal power plant design is prepared. All the parameters that feature in order to develop the power plant are considered and a numerical model is developed. The equations are solved with the help of the computer program written in FORTRAN. The grid independency and time step independency analysis are also performed.

A financial analysis report is prepared in order to revert back the system conditions if they are not economical. After obtaining the initial conditions the system design is developed by considering all the other parameters and performing simulations based on each condition. The optimal conditions are considered in each case to improve the system

design. Sensitivity analysis is performed with respect to the system design and the cost analysis. The best possible and the most economic conditions are considered and thus an economical system is developed with respect to the required conditions.

Structure of thesis

The structure of the thesis basically imitates the aims and objectives of the system.

In Chapter 1, Introduction, a general view about the geothermal power plants is given. The different types of geothermal power plants used around the world, the different techniques used in geothermal power plants, their need and their use are discussed. As drilling plays an important role, a small section talks about drilling techniques.

Chapter 2, literature review, discusses about the previous and related studies similar to such a system. This gives us an idea about the existing geothermal power plants and also various studies under various conditions.

Chapter 3 demonstrates the system design, the numerical equations and numerical model, typical output power, demand curve and all parameters involved in developing the system. Basically, this chapter is a bench mark moving forward in conducting experiments.

Chapter 4, talks about the financial analysis. The financial report keeps a check of the cost and also determines if the system is economical or not.

In Chapter 5, a number of numerical simulations are performed in order to test the sensitivity of the system. All the numerical results are shown obtained through the sensitivity analysis. The system performance is analysed.

Finally, some concluding remarks complete the study in Chapter 6.

Chapter 1: Introduction

Environmental changes and advancements in the use of technology around the globe have allowed humans to use electricity for almost every purpose in their day to day activities. The need for electricity has led to different techniques for its production. One such form of electricity generation is the geothermal power plant system. Geothermal power plants help to produce electricity which can be supplied to households, industries, companies, and other purposes.

The word "geothermal" means "Earth's heat". It comes from Greek, where geo means Earth and thermo means heat. As the heat generated from the Earth is known to be geothermal, the word is termed as Earth's heat [1]. With the increasing population and its needs around the world, a large number of people (2 billion), which is a third of the world's population, do not have access to modern services. A major issue is to improve the standard of living and provide required services for the poor. As one knows that the world's population is expected to double by the end of the 21st century, it is important to make clean energy available. Energy affects every aspect of modern-day life. A perfect

combination of energy use per capita in a country, life expectancy, and productivity in a country is essential [2].

Geothermal energy is also termed as a renewable source of energy. The Earth's natural heat is sustainable and is the thermal energy contained in the rock and fluid of the Earth's crust. The temperatures in geothermal power plants can go as high as 240^0C based on the depth and location of the power plant. The thermal energy extraction depends on the amount of heat or steam generated based on the amount of electricity required.

The production of electricity using geothermal power plants began in the early 20^{th} century. As the technology improved over the years, a number of changes and developments took place in order to design a model or system that helps in producing more energy at an economical cost. Some of the sources of geothermal energy within the Earth are radioactive decay and presence of volcanoes, hot springs, etc. which are essential for the generation of thermal energy. The thermal energy can be further converted into electricity with the help of organic rankine cycle machines (ORC) or turbines.

It is very important to have a good knowledge about the development and management of a geothermal power plant. The performances of the geothermal power plants in the past have been successful but not as efficient as one have expected them to be. By designing such new forms of geothermal power plant one can try to improve the cost and economic feasibility and power generation rate of the system. The need for better systems and designs has been increasing due to the development of technology. A system with more power generation with less cost and efficient time is always a need. So, it can be

considered that the present system might be economically more feasible and has better performance than the older systems.

The hydrological characteristics of the power plant or reservoir are very important. The re-injection of waste geothermal fluid was one technique developed and used through the knowledge of hydrology [3]. Earlier, the operational method was started purely as a disposal method but it was proved theoretically and practically that re-injecting the fluid back into the reservoir increases the longevity of the geothermal resources [3]. It is also known to improve the amount of energy extracted from the reservoir or power plant.

The re-injection method is a multi-parameter method and seems to be promising. Any method, regardless of how promising it seems has its positive and negative sides. So, a good knowledge of the following characteristics is essential for success.

a. Chemistry of geothermal fluid
b. Water-rock interaction
c. Geothermal reservoir engineering
d. Mechanical engineering.

The oldest and the first geothermal power plant ever used was built is Lardarello, Italy in the early 20th century. This geothermal power plant was effective in powering electric railroads in 1904. The system consists of hot granite rocks very close to the Earth's surface, which seems to be unusual, but it produces steam as hot as 220^{0}C (396^{0}F) [1]. It serves approximately a million houses in Italy.

Figure1.1: First geothermal power plant in Italy [1]

Figure1.2: Plant view and working employees - 1st Geothermal Power Plant (1904) [1]

The use of geothermal power plants and the production of electricity in an economical way have brought the attention of many countries around the world. This has led the way, and several countries have started using geothermal power plant systems for generating electricity [4]. The amount of electricity generation varies from 1 MW to 5 MW, depending on the infrastructure provided, cost, size of power plant, soil, rock type, etc.

The use of geothermal systems has grown strength by strength, and about 7,000 MW of energy is now produced in 21 countries around the world. The energy used in Northern California is produced by the 28 dry steam reservoirs present at The Geysers dry steam fields [4]. These dry steam power plants can produce as much as 2,000 MW of electricity at peak production. This is twice the amount of electricity a large nuclear power plant can produce. The dry steam power plants do not pollute the air with toxic gases, but emit only excess steam and very minor gases [4].

By using geothermal power plants, the US produces 2700 MW of electricity from geothermal energy, which is comparable to 60 million barrels of oil per year [4]. Below is the list of the regions and countries that have been using geothermal power plant systems in order to generate electricity and supply hot water for their households:

South American Andes, Central America, Mexico, the Cascade Range of the U.S and Canada, Alaska, parts of Russia, Japan, the Philippines, Indonesia, New Zealand, the Hawaiian Islands, the Rift valleys of Africa, the Mid-Atlantic Ridge, etc.

The advantage of using geothermal energy to generate electricity has been useful to a large extent for commercial, industrial, and household activities. A few advantages related to geothermal electricity are listed below.

- Environmentally friendly
- Reliable
- Flexible
- Cost-effective
- Helps developing countries to increase their economies and grow their communities.

1.1 Working pattern of geothermal power plant

The purpose of developing a geothermal power plant is to capture the thermal energy from the Earth's crust and convert it into electricity. It is known to be environmentally friendly and also cost-effective when compared to oil and gas wells. The oil and gas wells are built at higher costs when compared to the geothermal systems and also pollute the environment by releasing toxic gases and chemicals which might deplete the ozone layer. This is an environment drawback [5].

The working pattern of a geothermal power plant is unique and has an effective method of generating energy. Heat from the Earth's crust flows outward and is conducted through the surrounding rock (the mantle). As the temperature and pressure increase, the mantle converts into magma. The magma, which is lighter than the surrounding rock,

moves up slowly, carrying the heat from below, where the temperatures can be as high as 370 degrees C [5]. Water is injected into the well and flows around inside the well to become heated. The temperature in the ground increases as we go deeper into the Earth. Once tapped, these systems can provide the power plant with water and steam hot enough to generate electricity [5].

Geothermal power requires no fuel and is therefore immune to fuel cost fluctuations, but capital costs tend to be high. Drilling accounts for over half the cost, and exploration of deep resources entails significant risks. The amount of energy generated from a geothermal power plant is highly useful where a large power plant can supply electricity for an entire city or a small power plant can supply a rural village.

1.2 Closed loop versus open loop geothermal systems

There are two major forms of geothermal systems, the closed loop system and the open loop system. The design of these systems is not the same, but the working pattern is considered to be similar; however, there are some major differences. The closed loop systems are considered to be more efficient as they go deeper, and they are environmentally friendly. The performances of both these systems are discussed below.

1.2.1. Closed loop systems

The closed loop geothermal system is considered to be an advancing geothermal technology which helps in improving the power generation rate and efficiency of the

Earth's energy. It is also used to reduce to the cost and timeframe of power plant implementation. The closed loop systems require very little water, create no water pollution, produce renewable power with minimal carbon footprint, and have a very limited visual impact. The major advantage of the closed loop system is that the ground water chemistry does not affect the piping system.

The closed loop system consist of two loops: the primary refrigerant loop exchanges heat with the secondary water loop that is buried underground. The secondary loop is typically made of high density polyethylene pipe and contains a mixture of denatured alcohol and methanol [6]. Closed loop systems need a heat exchanger between the refrigerant loop and the water loop as well as pumps in both loops. These systems have lower efficiency than direct exchange systems, so they require longer and larger pipe to be placed in the ground. This increasing the excavation costs. Fig. 1.3 explains the process and functioning of a closed loop system.

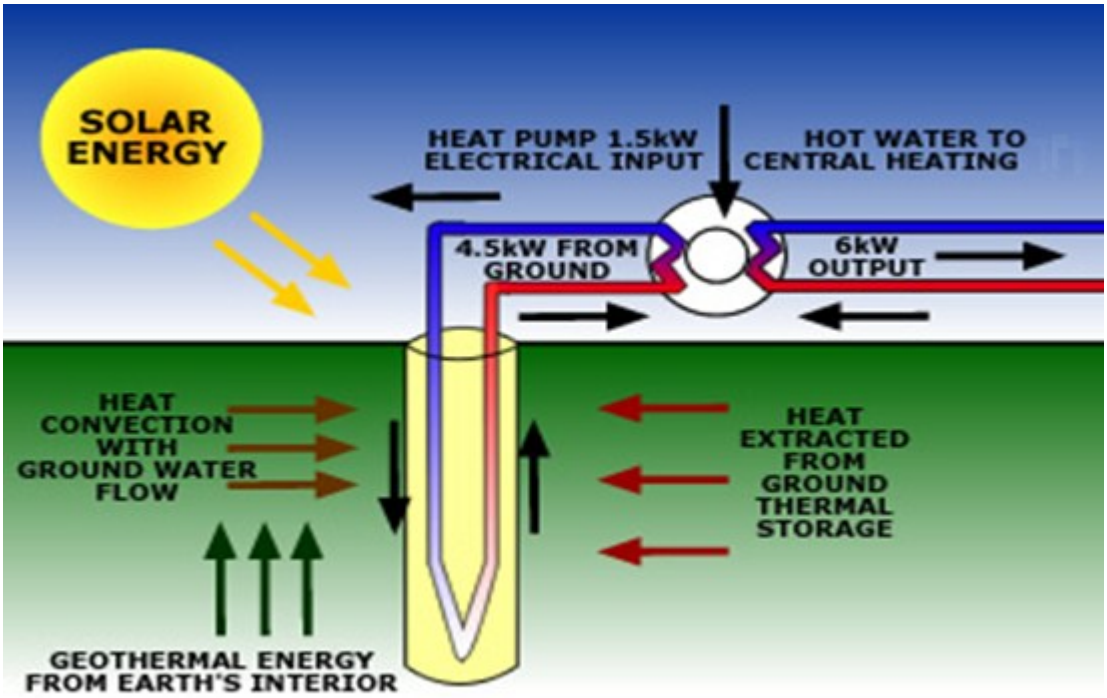

Figure1.3: Closed loop system with power cycle [7]

In this research, it is proposed to use heat pipe (which is explained in the following) instead of regular pipe to absorb and transfer thermal energy. The fluid in the heat pipe reaches a point where it is converted into gas or steam, and this steam is transferred to the surface. The heat pipes help in collecting the steam, and the fluid in the heat pipe drops back to the hot area. By the use of turbines or ORC, the thermal energy is converted to electrical energy, or electricity.

Heat pipes are considered to be very effective in a geothermal setup, as they help in heat transfer/ transport to the surface. A typical heat pipe consists of a sealed pipe or tube made of a material with high thermal conductivity such as copper or aluminium at both hot

and cold ends [8]. A vacuum pump is used to remove the air from the empty heat pipe and the pipe is later filled with a working fluid chosen to match the operating temperature.

The heat pipes have a cyclic thermal process where the working fluid evaporates to vapour by absorbing thermal energy. The vapour migrates along the cavity to the lower temperature end, which condenses it back to fluid, and it is absorbed by the wick, releasing thermal energy. The working fluid flows back to the high temperature end, and thus the cyclic process continues. Fig. 1.4 demonstrates the working pattern and design of a typical heat pipe.

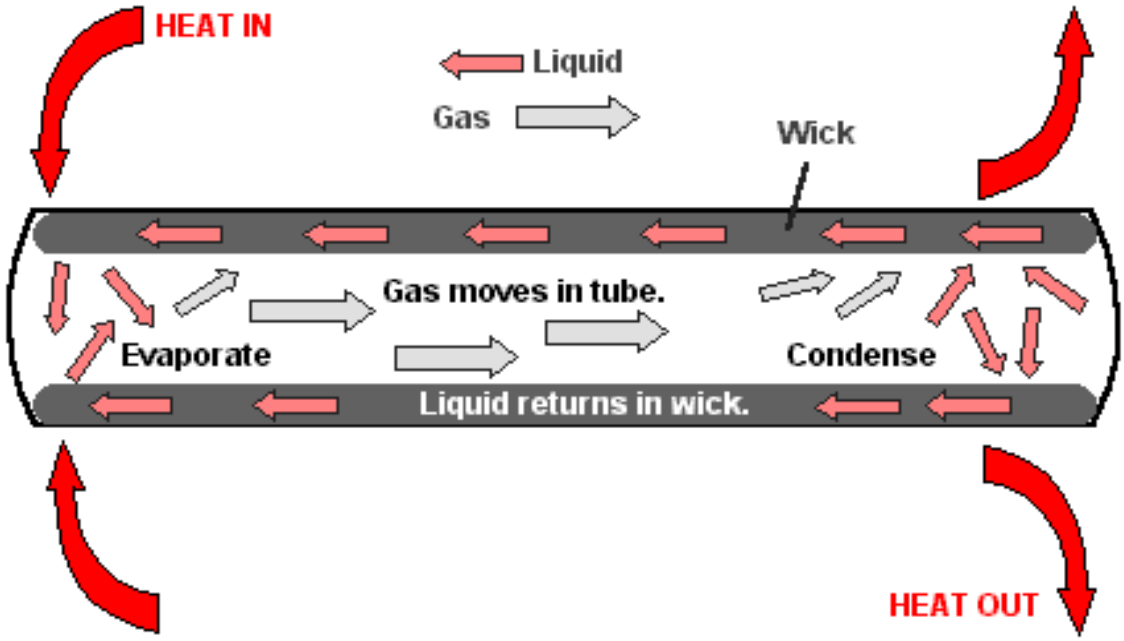

Figure1.4: Typical heat pipe design [9]

1.2.2. Open loop systems

Open loop systems are also known as groundwater heat pumps. In these systems, the secondary loop pumps the natural water from a well or body of water into a heat exchanger inside the heat pump. An injection well is used where the heat is either extracted or added by the primary refrigerant loop. The water is returned to the separate injection well. The water chemistry is not controlled in the case of open loop systems.

Open loop systems are considered more effective when they utilize the ground water because they have better coupling with ground temperatures. However, open loop systems are not preferable when the water contains high levels of salt, minerals, bacteria, hydrogen sulfide, etc. The drawback with open loop systems is that they are known to drain contaminants into aquifers, which is not environmentally friendly. Hence, more environmentally friendly techniques like the injection well are used.

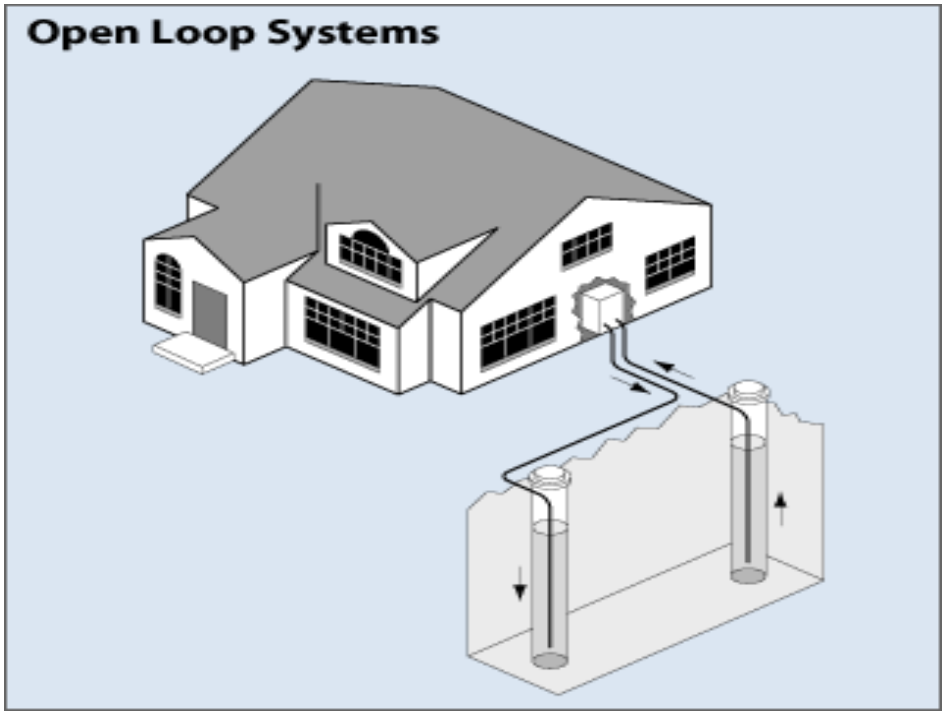

Figure1.5: Open loop system [10]

1.3. Geothermal power plant types

A geothermal power plant generates power by making use of geothermal energy. Geothermal energy production is extremely environmental friendly and is used in volcanic/geothermal locations around the world. This type of natural energy production system is used for producing large amounts of electricity, which can be essential for different purposes. It is also a cost-effective process, and no external source of monitoring or equipment is required to run the systems.

As mentioned previously, the electricity generated from geothermal energy is known as geothermal electricity, and it is a form of energy which includes three different

types of systems: namely, dry steam power plants, flash steam power plants, and binary cycle power plants. There are a number of countries which are implementing the techniques of geothermal heating and electricity, making huge steps forward [11].

The initial investment for the system design and the associated costs is another major aspect of geothermal systems, some of which include labour cost, cost of materials and equipment required, cost for construction of the power plant, the cost of land, etc. The one which involves the highest cost for setting up a geothermal energy system is the cost of drilling.

There are several types of geothermal power plants used across the world, some of which are known to be more effective than others. As mentioned previously, of all these, three methods are considered the most efficient and commonly used. They are:

i. A dry steam reservoir which produces steam but little water
ii. A geothermal reservoir that produces mostly hot water (called a hot water reservoir), used in flash power plants (T = 150-370 degrees C)
iii. A reservoir with T between 120-180 degrees C, not enough for flash steam but enough to produce electricity in binary power plants [11]

1.3.1 Dry steam power plant

The performance of a dry steam power plant can be achieved by minimizing or zeroing the interaction between the geothermal steam and water. The most effective use of

the system is seen by completely eliminating the mixing of geothermal steam and water. This can be achieved by having deep wells and collecting the superheated steam. The temperature of the superheated steam can go as high as 350 ^{0}C [12]. This superheated steam is transferred to the surface at high speed and then gets converted into electricity with the help of turbines. The dry steam reservoir uses the water in the Earth's crust and coverts it into steam after being heated by the mantle. The steam is then released through the vents. In the case of simple power plants, the efficiency of the turbine is improved by passing the steam through a condenser to convert it into water, which avoids environmental problems caused by the release of steam into the atmosphere. The reinjection wells are helpful in returning the waste water to the ground [12].

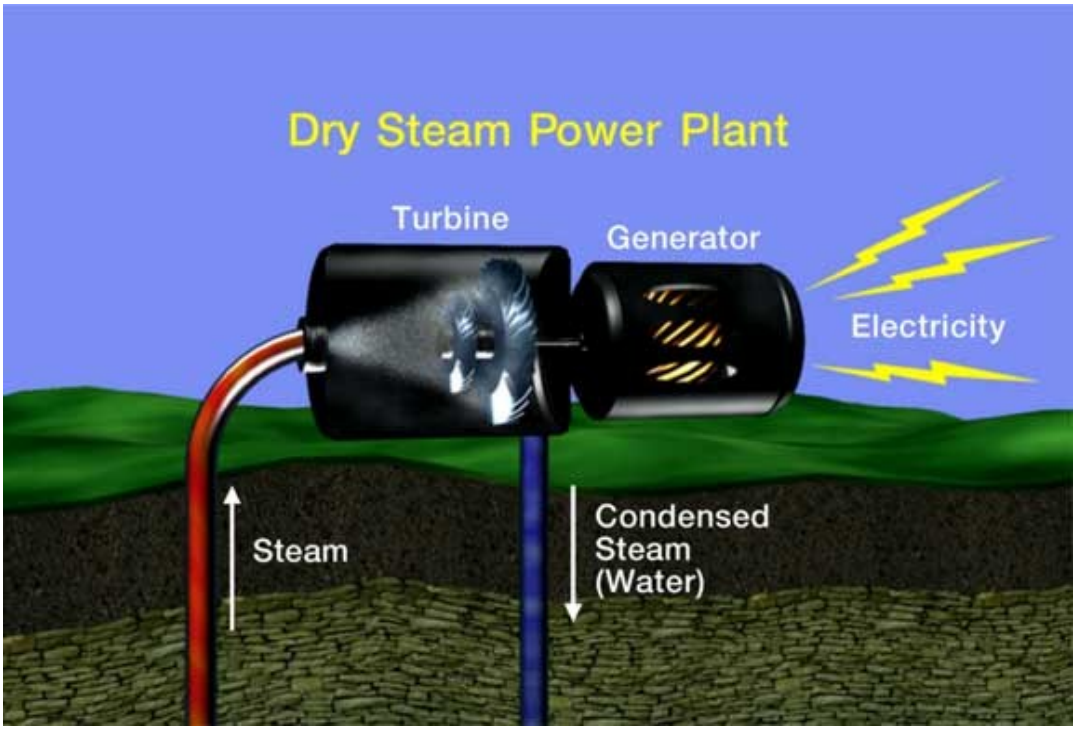

Figure1.6: Dry steam geothermal power plant [13]

Geothermal energy is considered a renewable resource. When rain falls, the underground reservoirs are refilled, and eventually the rainwater soaks into the crust of the Earth and the process continues.

The dry steam geothermal power plants are considered to be one of the earliest forms of geothermal power plants in North America. One such example is 'the Geysers' dry steam power plants in Northern California. This system depends on high temperature steam formation to directly provide energy in order to run the power generator turbines. This type of formation is called 'dry steam' [12].

1.3.2 Flash steam power plant

The basic principle of the flash steam power plant is the accumulation of hot water released from a flash tank. The accumulated liquid is flashed in order to convert the liquid into steam. This steam is later separated from the liquid and is used to run the turbines. Flash system power plants are generally useful when there is a liquid hydrothermal resource with a high temperature (> 350 F) [14].

To obtain better performance of the system, it is essential to set the injection well deep into the Earth, so that it reaches the subterranean rocks which are at a higher temperature than the boiling point of water. Water is than pumped deep into the injection wells with the help of a ground water pump using the flash steam power plant system. The

water filters through the rocks and rises back up through the nearby production well at a high temperature. This hot water from the production well enters a flash tank which reduces pressure and causes the water to boil rapidly or flash into vapour [14].

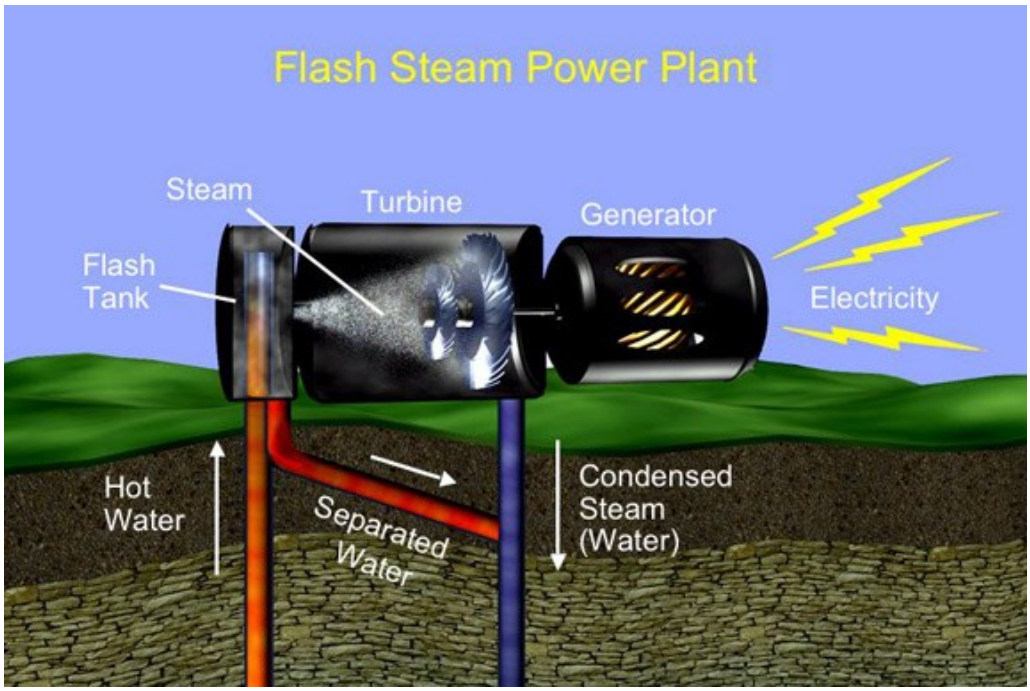

Figure1.7: Flash system power plant [15]

The water that comes from the flash tank is sent back to the ground water pump to be forced down into the Earth again. A steam turbine is driven by the vapour from the flash tank, which turns the shaft of an electric generator, and a condenser is used to cool the steam later. This converts the water vapour to a liquid state, and this liquid, along with the water from the flash tank, is forced by the groundwater pump back down into the Earth. A certain amount of this condensed vapour serves for drinking and irrigation purposes since

it is distilled. The monitoring of the flash tank must be done in such a way that flushing and cleaning is carried out in order to clear the materials. The flushing must be done more frequently when the mineral content in the liquid is high [14].

1.3.3 Binary steam power plant

The binary steam power plants heat a fluid which has a boiling point less than that of water by using high temperature geothermal water. When the hydrothermal resource is of a lower temperature (100 F), this technique is employed [16]. The hot water is passed to a heat exchanger where it is compounded with a secondary liquid with a lower boiling point (like isobutene or izopentane).

A two-step process is used here in order to extract power from geothermal water which is not hot enough to produce steam for the turbine. The water from the geothermal reservoir uses water-based geothermal resources of approximately 200-360 degrees F [16], since, it never comes into direct contact with the blades of the turbine generator. Warm geothermal water is pumped to the surface and passed through a heat exchanger in the binary cycle system, where the heat exchanger contains a fluid such as butane or pentane hydrocarbon with a much lower boiling point than water. This secondary or 'binary' fluid flashes into vapour due to the heat from the geothermal water. The vapour created by heating the pentane helps to spin the turbine powering the generator, while the cooled steam from the geothermal source is injected back into the formation where it heats up again and eventually re-circulates through the heat exchanger. Hence, it can be said that

geothermal energy is considered a renewable resource, as a properly managed formation can potentially produce power indefinitely [16].

The binary steam power plants are more common nowadays, since most of the resources are at lower temperatures.

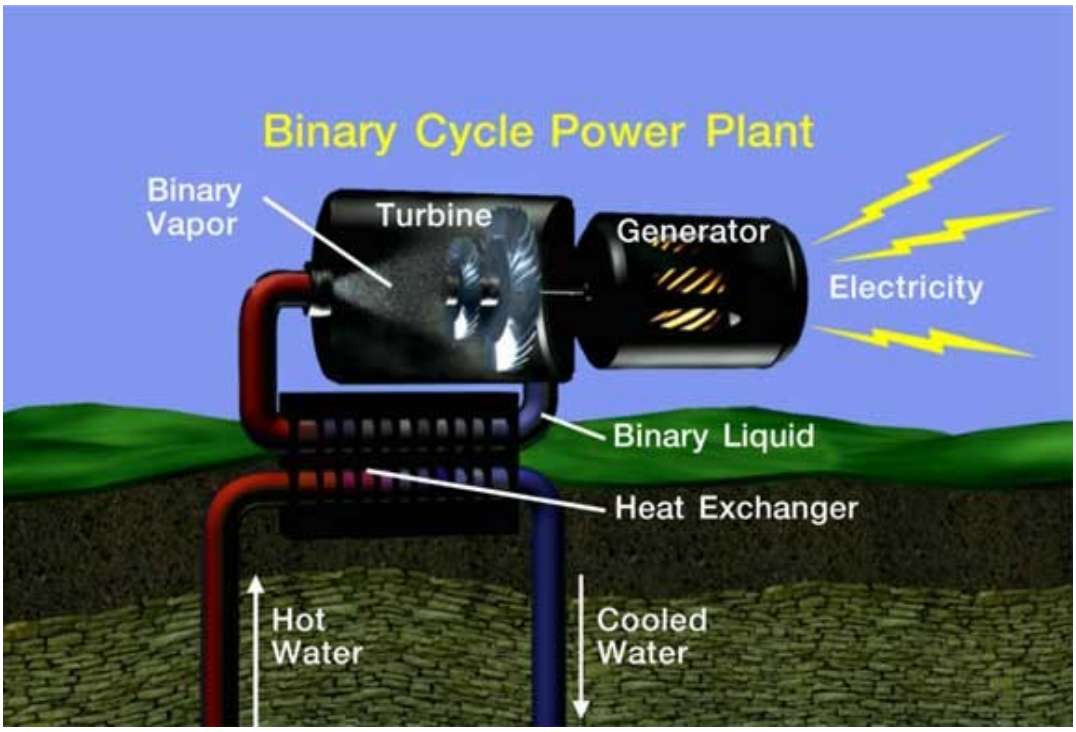

Figure1.8: Binary steam power plant cycle [17]

Moderate-temperature geothermal water is much more common than high-temperature water, and many areas have been identified as having geothermal reservoirs with water that is below 400 degrees F (204 C) [16]. The US Department of Energy predicts

that most geothermal power plants built in the future will be binary cycle power plants that can take advantage of this slightly cooler water.

1.3.4 Hybrid power plant

Boiling water as well as steam is produced by some geothermal fields which are used in power generation. In order to make use of both steam and hot water, in this system of power generation the flashed and binary systems are combined. Hybrid power plants, however, have lower efficiency compared to that of dry steam plants [18].

1.4. Different uses geothermal energy

The massive amount of energy produced through geothermal power plants is used in creative ways, and its use only limited by our ingenuity. During olden days, geothermal water was used freely for relaxing in warm waters, and the Romans used it to treat eye and skin diseases [19]. In a few other places, people started using it for commercial and household purposes, like the New Zealanders and the Aboriginal people, who used water for cooking and medicine.

France and Italy were two of the earliest countries to start using geothermal energy to heat their homes. Thereafter, people around the world started using geothermal water

for other purposes, such as cooking, household services, heating, etc., and the use of geothermal water and energy came into force around the world. Nowadays, geologists, geochemists, drillers, and engineers are exploring in order to locate new underground areas to obtain geothermal water.

The uses of geothermal water have been increasing, and some simple and effective ways in which it can be used are:

- ✓ For heating individual buildings and small districts
- ✓ Aching muscles
- ✓ To help grow flowers, vegetables, and other crops
- ✓ Shorten the time needed for growing fish, shrimp, etc.
- ✓ Pasteurize milk, dry onions and lumber, and wash wool

Geothermal heating systems are used in districts where it hot and clean water can be pumped into the city. The world's largest district heating system is located in Reykjavik, Iceland. Geothermal energy is its main source of heat, and it has become one of the cleanest cities in the world [19].

1.5. Drilling technologies

Drilling systems and technologies play a very important role in designing a geothermal power plant. To go as deep as possible into the Earth in order to run a

geothermal power plant, one needs proper drilling techniques, and a few of the latest drilling techniques have the capacity to go as deep at 5,000ft – 10,000ft deep.

The exploitation of the geothermal deposits is divided as:

i. Hot steam deposits

ii. Thermal water deposits

iii. Hot dry rock (HDR) [20]

Hot steam and thermal water sources can be used directly for heating purposes or to generate electricity. If the underground surface consists of just hot rock, this can heat up cold water that is injected into it.

Simply drilling down is not enough for a geothermal power plant. It needs high-grade or high-end resources which have features that can be easily exploited, high average thermal gradients, high rock permeability and porosity, sufficient fluids in place, and an adequate reservoir recharge of fluids [20].

Recent studies and trends have suggested that it is time to consider 'engineered' or 'enhanced' geothermal drilling techniques. A number of new drilling techniques have been implemented, but the most useful and efficient ones are discussed below.

1.5.1 Diamond drilling

Diamond-cutter drill bits cut through rock quicker, reducing the cost of drilling for energy resources. The basic principle of diamond drilling is that it is done with diamond bits, which help in drilling the outer portions of the surface, and the core is collected

through pipes or tubes provided in the system. This technology works with the assistance of very powerful and effective diamond bits. These bits need to be reloaded at certain intervals of time with respect to depth from the surface. On average, a diamond bit can serve from 500ft – 800ft.

The polycrystalline diamond compact (PDC) drill bit is one important form of drill bit that was introduced by General Electric Company (GE) in the 1970s. The PDC bit uses thin diamond layers bonded to tungsten carbide-cobalt studs or blades. The shearing action of the drill cutter bits is possible due to the extreme resistance of diamond to abrasive wear. These PDC bits are considered to be more efficient than the crushing action of roller-core bits. [21].

Figure1.9: Diamond cutter drill bit [21]

The PDC process works very effectively and can drill more than 2,200 feet per hour, depending on the surface and the rock material. According to recent information from experts from different diamond drilling companies, it is observed that the cost of drilling is about $100- $120 per foot to drill a surface using the diamond drilling technique [21]. The reason for the process to be used is the effectiveness and time frame to drill a certain surface.

Table1.1: Drilling factors and their performances [21]

Components	Range (units)
Size of bit	2 7/8" to 12 ½"
Depth	5000 feet to 10000 feet deep
Efficiency	5 to 10 foot continuous retrieval of core sample
Cost	$ 80 to $ 120 depending of the surface and angle of drill
Angle of drill	90 degrees, Can even take up different angles.
Bit efficiency	500 ft. – 800 ft. depending on the surface of the rock.

1.5.2. Rotary steerable PDC drill

Rotary steerable PDC drill bits are custom-designed for every directional application and type of system, including vertical automated and rotary steerable push-and point–the-bit systems. These directional drill bits deliver the right amount of steerability, walk rate, and torque control for the application, while minimizing the effects of damaging down-hole vibration.

Conventional directional drilling utilizes a bent housing motor or bent sub in order to deflect the bit in the desired direction. This type of conventional drilling requires drilling to stop and start, which causes problems with hole cleaning [22]. Using a directional drilling well with a rotary steerable system results in a smoother wellbore, which results in a constant rotation and deflection of the drill string through adjustments down-hole.

The major use of such systems is seen in oil extraction industries, which need deep drills.

Figure1.10: Rotary steerable PDC drill sample [22]

Rotary steerable systems are revolutionizing the way in which oil and gas wells are drilled. Over the past 5 years the technology has emerged from prototype status to a standard application in locations with good infrastructure, like the North Sea or the Gulf of Mexico. In more remote areas with more challenging logistics, like West Africa, the Asia Pacific region, and South America, the use of rotary steerable technology has been very limited [22].

Finally, it can be summarized saying that chapter 1 gives all the basic knowledge about geothermal power plants its types and performances of each system. It also provides information about the drilling technologies and working pattern of different geothermal energy systems and also their uses to mankind.

Chapter 2: Literature review

Extensive research has been performed on shallow geothermal power plants as compared to deep geothermal energy systems, but deep geothermal systems have not been extensively studied so far. In the following, some recent studies are briefly reviewed.

2.1. Deep geothermal power plants

Research studies based on deep geothermal power plants are very limited when compared to shallow geothermal power plants. One such deep geothermal power plant system established in France is discussed below.

2.1.1. Geothermal electricity generation in Soultz-sous Forets

The European geothermal project in Soultz-sous Forets created the world's deepest geothermal heat exchanger. The key requirement for this was the idea of using large-scale existing fractures and the deep waters stored within them for the heat exchange process. As opposed to other geothermal power plants, this power plant is using natural hot water or steam sources and existing fractures up to a maximum of 175^0C in hot granite, which were expanded to a depth of 5000 meters [23].

This geothermal power plant is based on three deep bore holes. Two holes pump the hot water using down-hole pumps. Thee deep waters are corrosive and contain approximate 100gm/L of dissolved salts and gases, particularly N_2 and Co_2. The 3rd bore hole is used to reinject hot water back into the system [23]. The hot water here flows through the system of fractures in the rocks, heats up, and returns to the area of the extraction wells, where it is drawn in. This closed loop prevents negative effects on the environment [23].

Aboveground, the heat is transferred to an organic medium in a 2nd closed loop via tubular heat exchangers. This medium is expanded via a turbine with a connected generator and subsequently cooled and liquefied in an air-cooling system with fans. This special power plant process in called an Organic Rankine Cycle (ORC). To generate electricity, the ORC technology allows heat at a relatively low temperature level, approximately 90 ^{0}C [23].

Figure2.1: ORC system of a geothermal power plant [23]

At temperatures of 100 degrees C or less, geothermal water is not hot enough to vaporize water. A normal steam turbine using water as a work medium is not suitable in this case. An ORC system is used instead. A steam turbine also forms the core of this kind of system; however, instead of water, the steam turbine uses an organic material such as izopentane [23]. A heat exchanger transfers the heat from the geothermal cycle to the organic fluid. This material also evaporates under high pressure at temperatures lower than 100 degrees C.

Water can be circulated and heated via a geological heat exchanger through multiple bore holes. The thermal energy connected in this way can be used at the surface to generate electricity or to supply heat; this process is known as hot dry rock (HDR) technology [24]. The main advantage of this is that it can be applied in large areas,

independently of sources of water and steam. The temperature profile for this location is shown in Figure 2.2.

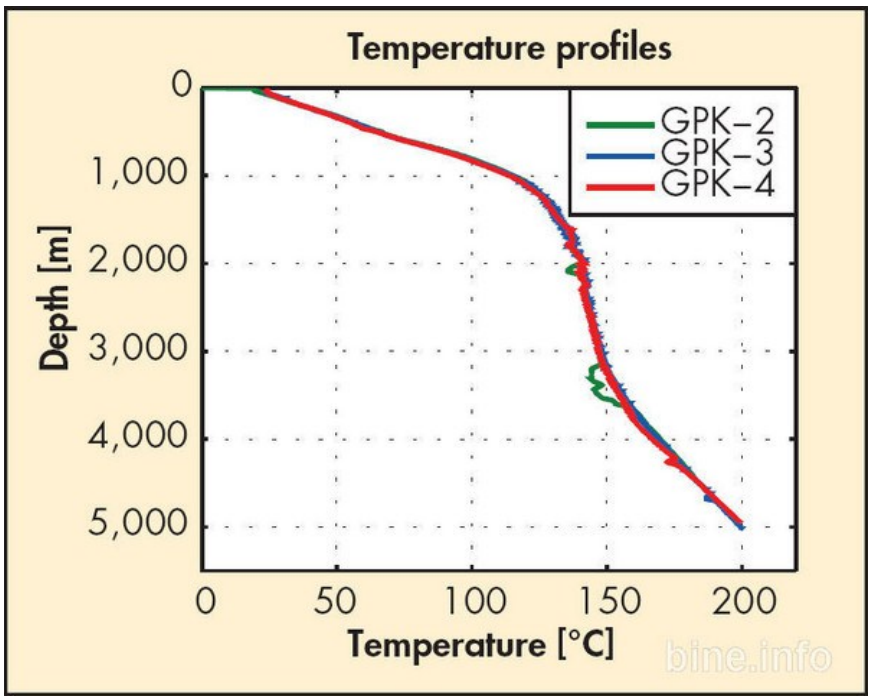

Figure2.2: Temperature versus depth profile [24]

The different parameters used for the system, including the expenditure, the grants, the length of the drill, the net production of electricity, etc. are given in Table 2.1.

The power plant has been able to produce nearly 1.5MW of electricity with an internal power consumption of 0.6MW [24]. The temperature was maintained around 70^0C for the reinjection of the water into the system. Table 2.1 shows all the results.

Table2.1: Results illustrating the performance of the system [24]

Incentives and grants	**€ 80 million**
Overall drill length	**20 km**
Volume of geological heat exchanger	**2-3 km^3**
Area of geological heat exchanger	**Upto 3 km^2**
Pumped water quantity	**35 l/s**
Pumped heat	**13 MW**
Temperature of pumped water	**175 ^0C**
Temperature of reinjected water	**Approx. 70^0C**
Gross electricity production	**2.1 MW**
Internal power consumption of the plant	**0.6 MW**
Net electricity production	**1.5 MW**

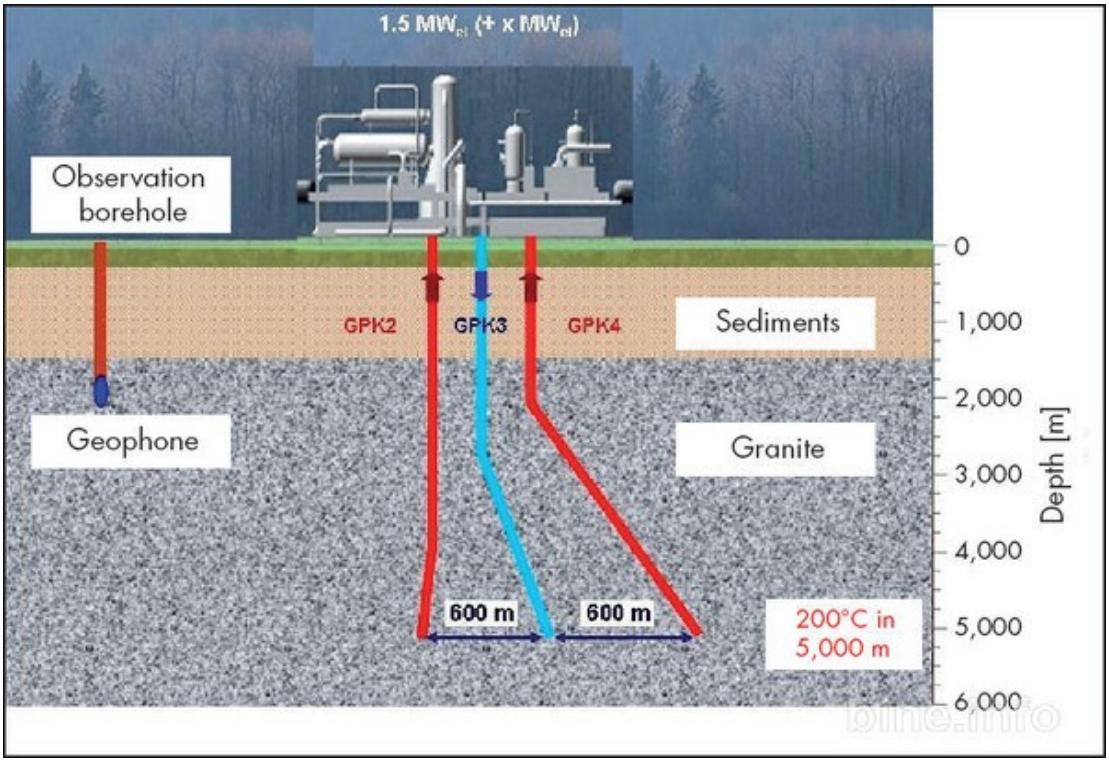

Figure2.3: Performance of the system at a depth of 5000m [24]

2.2 Shallow geothermal systems:

Diersch et al. (2010) proposed a finite element model for borehole heat exchanger (BHE) systems. They considered a shallow system where the depth was 100m. They compared different numerical and analytical results for a steady state condition and a given temperature [25]. The transport equation used is written as

$$\frac{\partial T}{\partial t} + u\frac{\partial T}{\partial z} - D\frac{\partial^2 T}{\partial z^2} + \varphi(T - T_s) = 0 \qquad (2.1)$$

where T= Fluid temperature in the in-pipe, u= refrigerant fluid velocity, ϕ= specific heat transfer co-efficient, z= vertical coordinate, T_s= vertical soil temperature, D= depth.

The analytical and numerical temperature profiles with respect to the depth were compared and plotted. The temperature profile for a transient BHE solution for a coaxial pipe system of annular inlet for laminar flow was compared to Heidemann's solution and plotted for all three conditions, and a good agreement was observed. Fig. 2.4 illustrates the typical results for a temperature profile for a BHE [25].

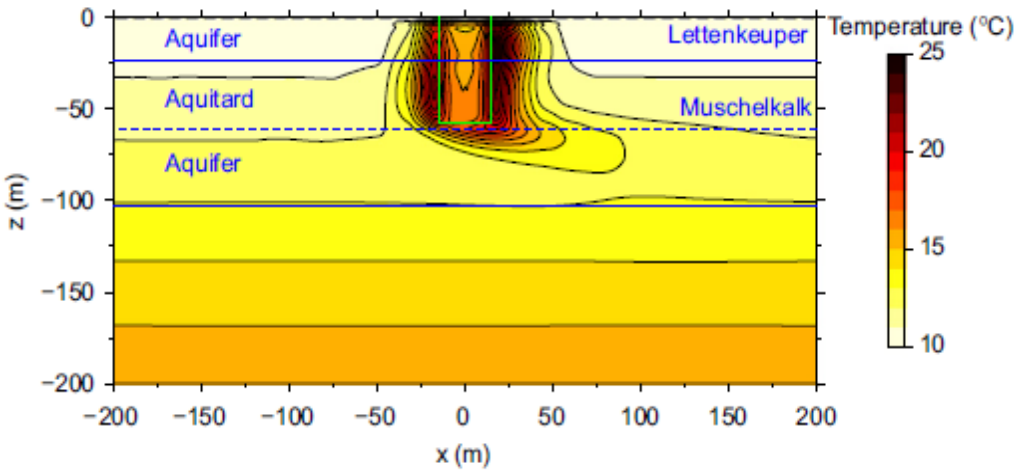

Figure2.4: Cross section temperature profile oriented to the main groundwater flow direction [25]

Ou and Einav (2010) discussed the fluid temperature and power estimation of geothermal power plants by a simplified numerical model. They discuss the control of power generation by the temperature of fluid flowing through the U-shape pipes. They

simulated the heat conduction, heat energy, and power production of the system [26]. The system design is shown in Figure 2.5.

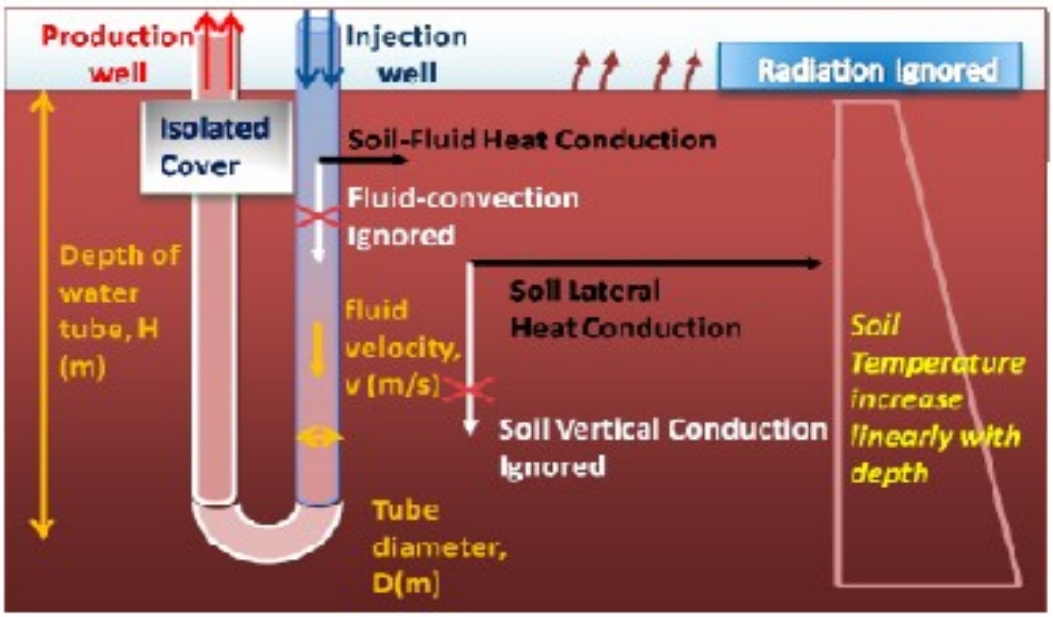

Figure2.5: A schematic view of a geothermal power plant U-pipe system [26]

The numerical results were discussed for different fluid materials like water and glycerol and the system design parameters such as water velocity and pipe depth. They showed that after a certain time, the temperature of both fluid and surrounding soil will reach a steady state. It was shown that the ultimate fluid energy will decrease with the rise of fluid velocity or pipe diameter, but will increase with the total pipe depth [26].

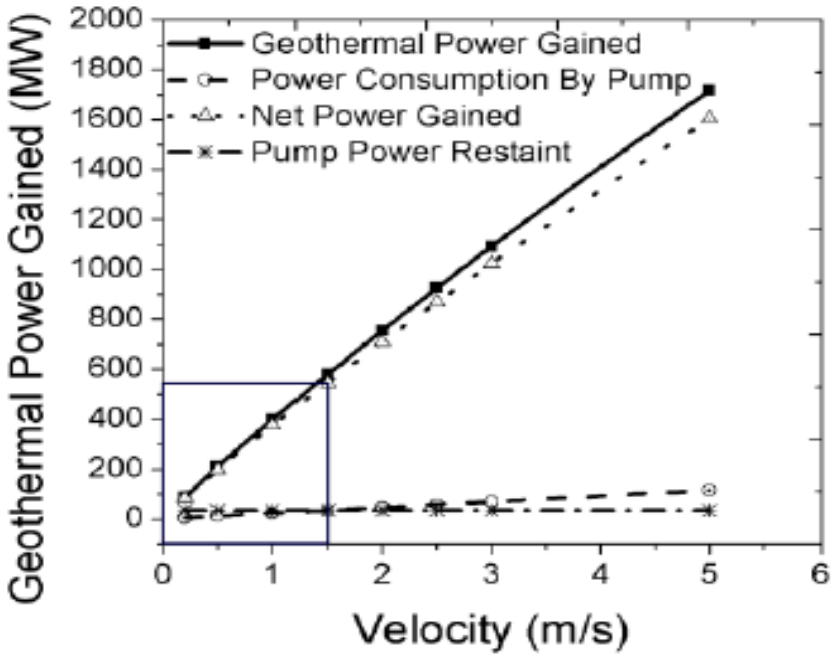

Figure2.6: Geothermal power gain versus velocity of the system shown in Fig. 2.5 [26]

Recently, using heat and mass transport equations, Mottaghy and Dijkshoorn (2012) implemented an effective finite difference (FD) model for borehole heat exchangers. They modeled a multiple borehole heat exchanger (BHE) using the general 3-D coupled heat and flow transport code SHEMAT [27]. In their model, the BHE with arbitrary length can be either coaxial or double U-shaped (Figures 2.7 and 2.8).

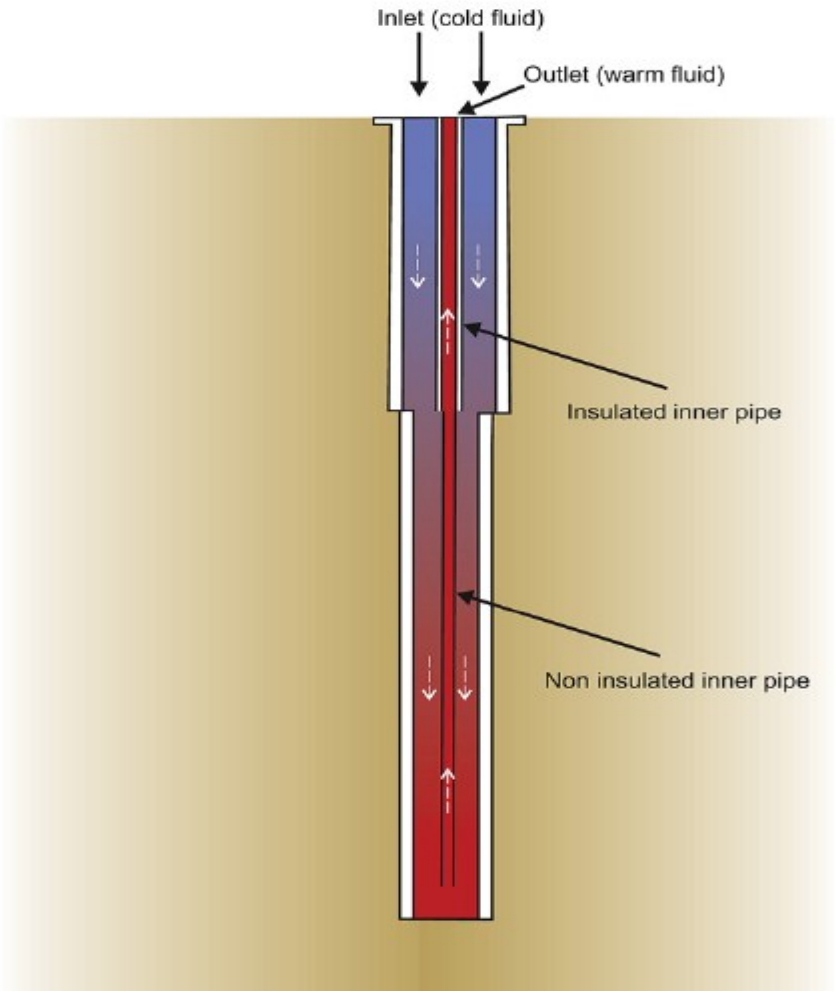

Figure2.7: Sketch of a deep BHE with varying pipe diameter [27]

Their semi-analytical approach involved the determination of thermal resistances of different parts of the BHE. The model considered the heat transport between the inner hot pipe and the outer cold pipe as well as the heat transport between the outer cold pipe and the soil as thermal resistances [27].

The formulation for the double U-shaped BHE was similar to the above approach, but the determination of thermal resistance was more complicated [27]. A typical computational grid as well as the temperature distribution is shown in Fig. 2.9.

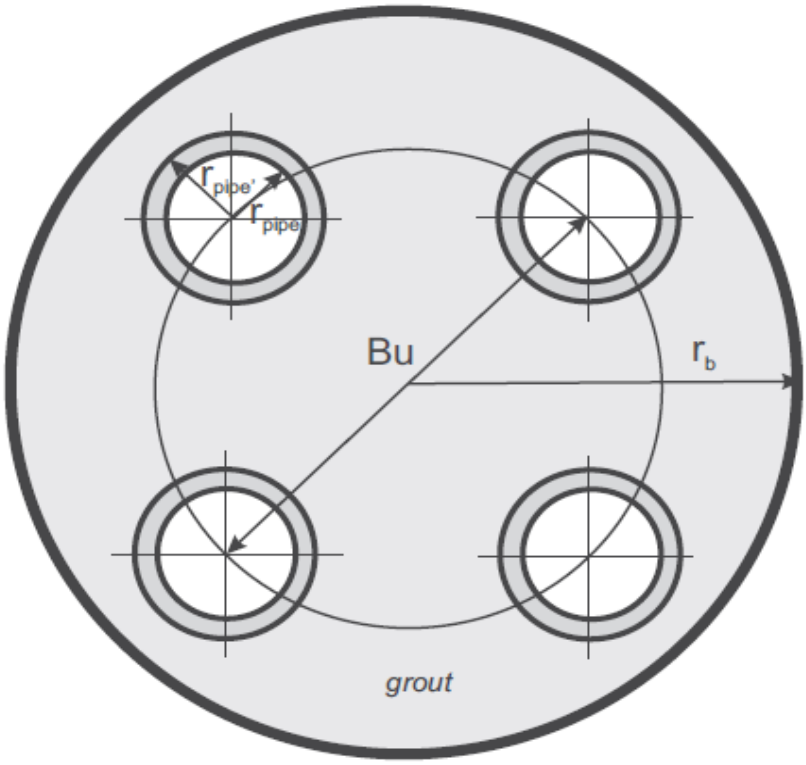

Figure2.8: Cross section of a typical double-U shaped BHE [27]

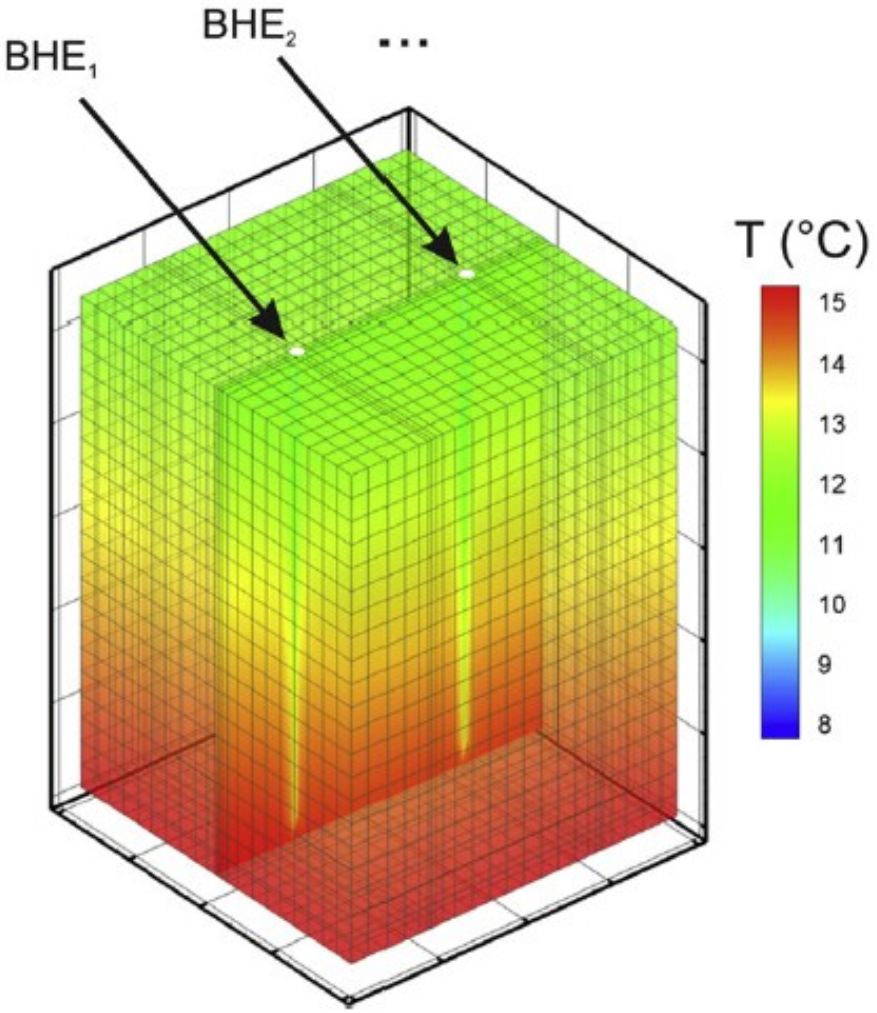

Figure2.9: Temperature distribution around two running BHEs which are extracting heat [27]

They concluded that the coupling of a finite difference formulation of BHE with the SHEMAT [27] model is efficient and accurate. Their approach can be used in any finite difference or finite element model. Thus, it is possible to consider an arbitrary,

heterogeneous geologic model as well as the influence of groundwater flow in the surroundings of one or multiple borehole heat exchangers [27].

Similar work related to borehole heat exchangers was performed by Lazzari et al. (2010), where they discussed the long-term performance of BHE fields with negligible groundwater movement. They considered double U-tube BHE fields investigated by finite element simulations. They used the COSMOL Multiphysics software package for areas in which the effects of groundwater movement are negligible [28]. The double U-tube BHE was considered with high performance polyethylene tubes in which a water- ethylene glycol 20% solution flows in homogeneous soil with an undisturbed ground temperature of 14^0 C (Fig. 2.10).

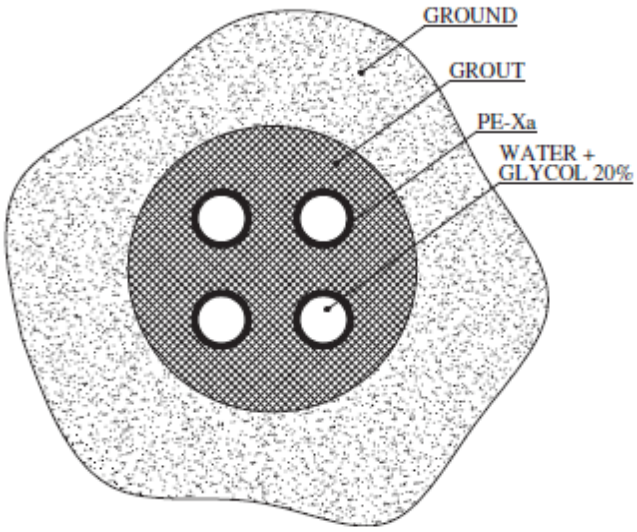

Figure2.10: Sketch of double U-tube BHE cross-section [28]

The long-term performance of double U- tube BHE fields placed in ground with negligible groundwater movement was studied. Six time-periodic heat loads with a period of 1 year were considered, with either full compensation, partial compensation, or no compensation for winter heating with summer cooling [28].

Ozgener and Hepbasli (2005) worked on the modeling and performance evaluation of ground source (geothermal) heat pump systems, which deals with the energetic modeling of ground source heat pump (GSHP) systems for their system analysis and performance assessment [29]. The analysis covers two GSHPs: namely, a solar assisted vertical GSHP and a horizontal GSHP. Some thermodynamic parameters, such as fuel depletion ratio, relative irreversibility, and productivity were investigated for each system [29].

Bauer et al. (2010) discussed the development and application of a transient three-dimensional (3D) analysis of a borehole heat exchanger model. Their model included the thermal capacities of the borehole components in order to consider the transient effects of heat and mass transport inside the borehole [30]. They used simplified thermal resistance and capacity models (TRCMs), and the results were compared to complex computations such as finite element (FE) models. They also compared the results with analytical solutions and showed the advantage of the developed 3D transient model [30].

Teza et al. (2012) analysed the performance of a long–term, irregular–shaped, borehole heat exchanger system with real pattern and regular grid approximation. They discussed the performance of the BHE and the patterns (e.g. rectangular, L-shaped, T-shaped, etc.) often used in the BHE fields. In order to evaluate the validity of the system, 25-

year time span simulations were carried out by 2D finite element modeling [31]. They also showed that a regular-shaped BHE can be reasonable under a no ground water flow condition or very minimal ground water flow, but if a heating or cooling imbalance occurs, the thermal footprint of a BHE can be very extensive. This would prevent the installation of future BHE systems nearby [31].

Valladares et al. (2005) discussed the numerical modeling of flow processes inside geothermal wells, which is an approach for predicting production characteristics with uncertainties. One-dimensional steady and transient numerical modeling for describing the heat and fluid dynamic transport inside geothermal wells was conducted [32]. A one-dimensional simulator, GEOWELLS, was developed for the study of fluid flow and heat conduction equations inside the geothermal well. In most of the applications, the simulation results provided by GEOWELLS were in good agreement with measured field data and supported by statistical analysis. They mentioned that additional experimental and computer work were required to include appropriate thermo-physical properties and to test the sensitivity of the approach [32]. They also stated that a comprehensive knowledge of errors will be obtained only if a large number of measurements are collected.

Paly et al. (2012) worked on the optimization of energy extraction for closed shallow geothermal systems using linear programming. They worked on shallow geothermal technologies that directly use the heat stored in the subsurface. The depth of the system was 400m, and heat pumps were applied to extract the energy. A closed ground-coupled GSHP system was used. Multiple adjacent borehole heat exchangers (BHEs) were installed which operate with variable energy loads [33]. The system model

demonstrated a simplified hypothetical case of 25 BHEs that were operated for 30 years. A seasonally variable heating system was set up to serve large office buildings, schools, etc. Figures 2.11 and 2.12 show the temperature change with respect to time for the working fluid of all BHEs [33].

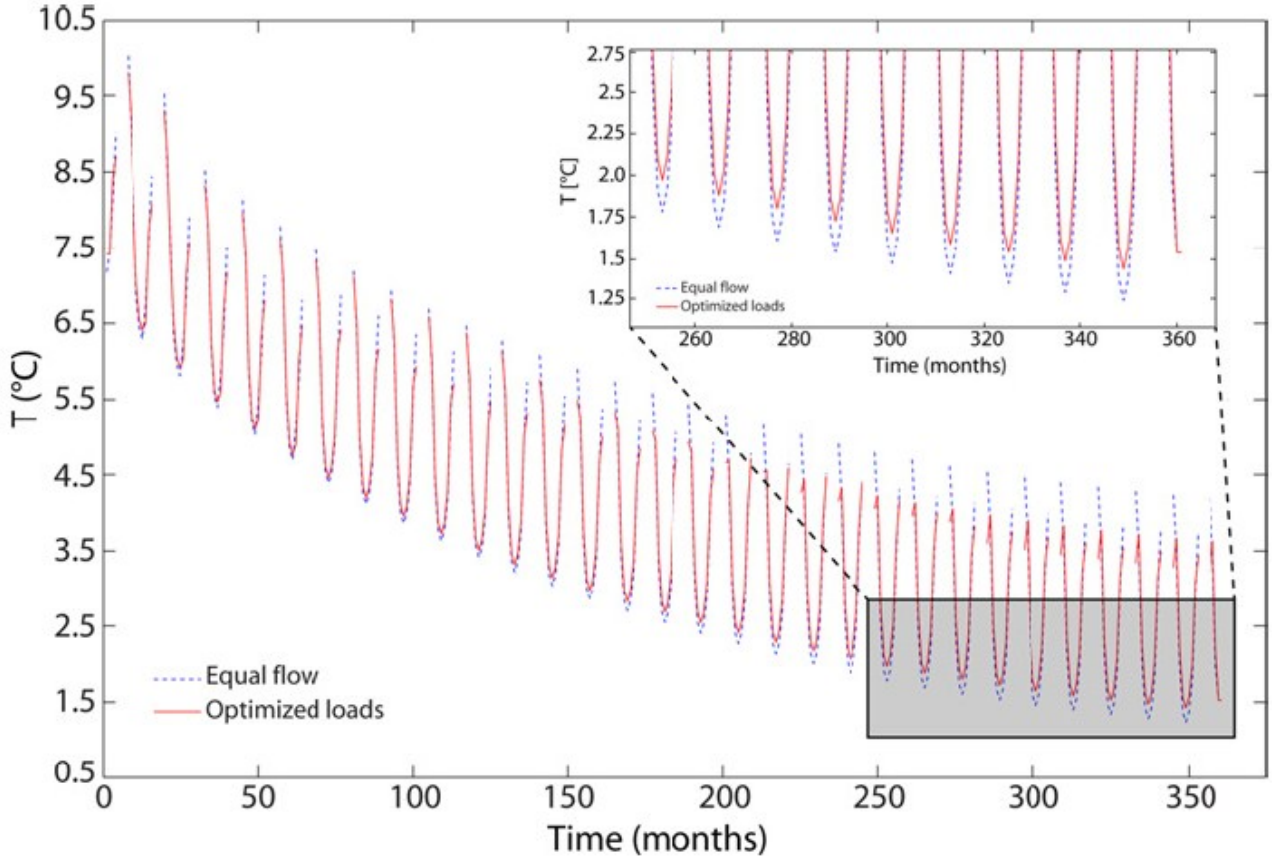

Figure2.11: Temperature (^{0}C) change versus time (months) [33]

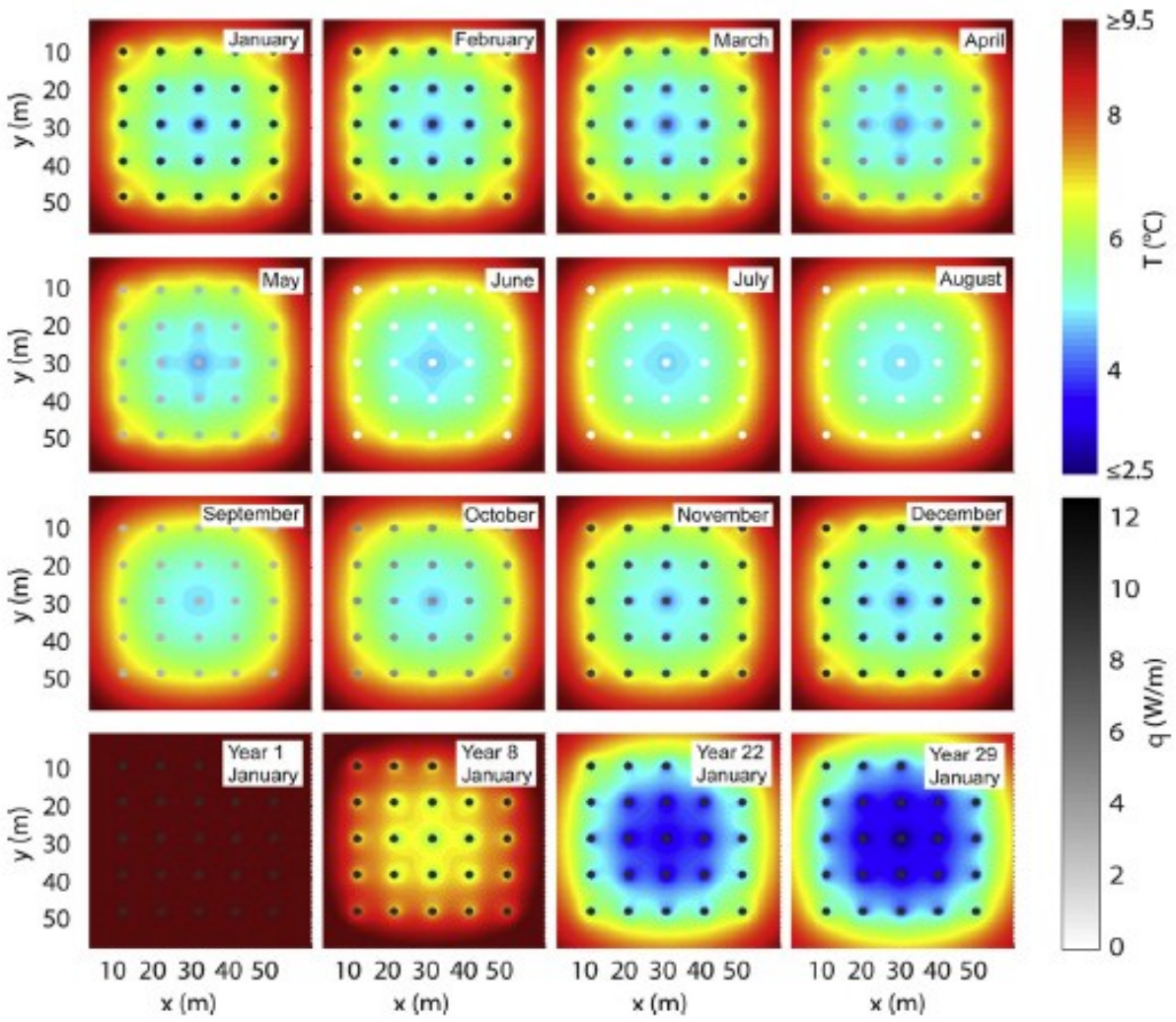

Figure2.12: Temperature distribution and BHE workloads for non-optimized equal load [33]

Meer et al. (2008) discussed the time-dependent shape functions for modeling highly transient conductive heat flow in geothermal systems. The shape functions were made adaptive by enhancing the approximation functions with time-dependent variables without adding an extra degree of freedom or applying mesh adaptation. An iterative method and an analytical method were suggested which enable the exponential and

explicit shape functions in each time step. The ability to capture high-gradient temperature profiles was illustrated using numerical model cases where large standard finite elements fail [34].

Zeng et al. (2003) worked on the heat transfer analysis of boreholes in vertical ground heat exchangers. The ground heat exchanger (GHE) is used for extraction or injection of thermal energy from/into the ground. They designed the model by considering the fluid axial convective heat and thermal short-circuiting among U- tube legs, and a new quasi-3D model was established. Fig. 2.13 demonstrates the system design [35]. The borehole thermal resistance is defined by the thermal properties of the construction material and arrangement of flow channels. Analytical expressions of the fluid temperature profiles were derived, and also the double U- tube and single U-tube boreholes were derived for different configurations. It was also observed that double U-tube boreholes are superior to those of the single U-tube with reduction in borehole resistance [35].

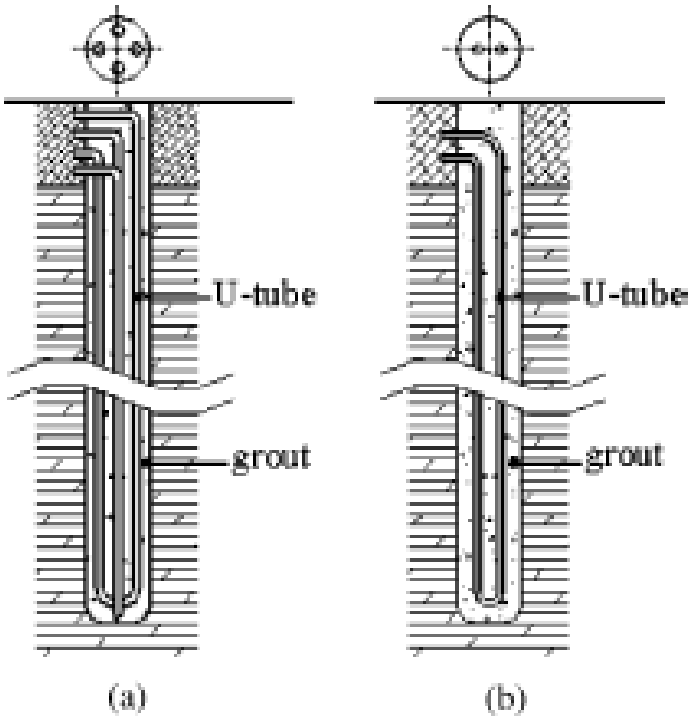

Figure2.13: Schematic diagram of boreholes in GHE. (a) Double U-tube and (b) Single U-tube [35]

The effective borehole thermal resistance was considered to be of great importance in heat transfer analysis of the GHE's. Zeng et al. (2003) presented a quasi-3D model with temperature profiles for all possible circuit layouts. Among all, certain parallel arrangements resulted in lowest resistance, and differences among them were negligible [35]. Fig. 2.14 illustrates the performance of borehole thermal resistance to thermal conductivity. They finally stated that the heat transfer models of the GHE boreholes and the expressions derived may serve as theoretical foundations in the performance simulation and economic analysis of GCHP systems [35].

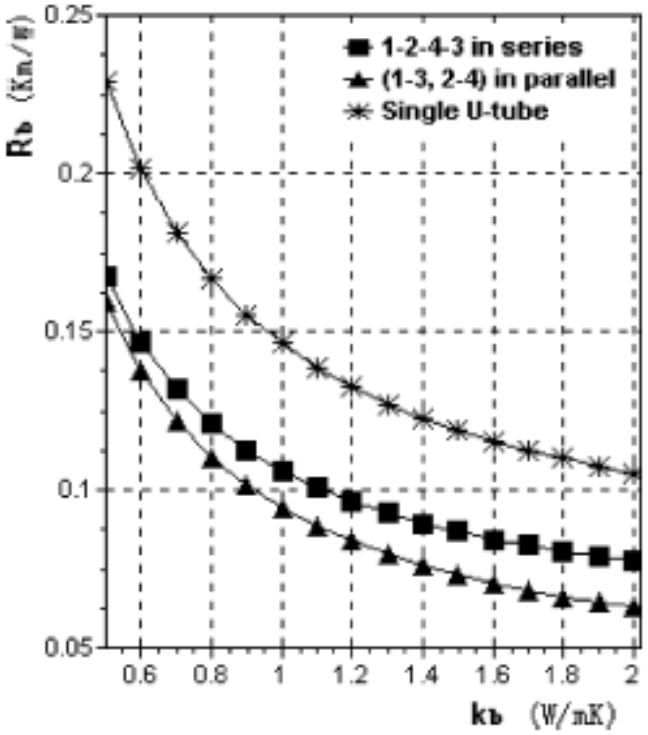

Figure2.14: Borehole thermal resistance versus thermal conductivity [35]

Yang et al. (2009) reviewed the models and systems of vertical borehole ground-coupled heat pumps (GCHP). GCHP systems are used extensively in residential and commercial buildings due to the attractive advantages of high efficiency and being environmental friendly. They discussed the applications of air-conditioning and various hybrid GCHP systems. It was observed that the GCHP technology can be used both in cold and hot weather areas and that the energy saving potential is significant [36].

Lamarche and Beauchamp (2006) proposed a finite line source model for geothermal boreholes. Heat transfer around vertical ground heat exchangers is a common problem for the design and simulation of ground-coupled heat pump (GCHP) systems. They

discussed a new analytical model that yields results very similar to numerical models and provides better flexibility for a parameterized design. They proposed a mathematical model to find the temperature distribution that satisfies the heat conduction equation by ignoring the angular dependence of temperature. The analytical solution has the advantage of being more flexible, especially in designing nonexistent systems where a parameterized approach is used to optimize the system. Fig. 2.15 shows the performance of different boreholes [37].

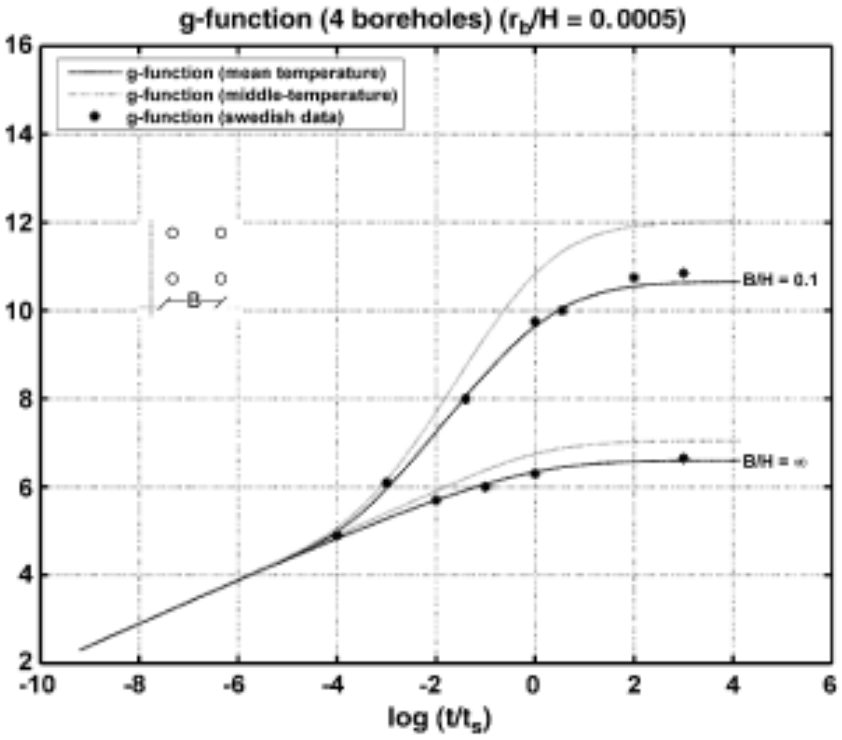

Figure2.15: Function for four interacting boreholes separated by a distance B [37]

Lim et al. (2006) discussed an experimental study on the thermal performance of ground heat exchangers. Thermal response tests were used primarily, not only for in situ determination but also for evaluation of grout material, heat exchangers, and ground water effects. Their main purpose was to determine the thermal conductivity and groundwater flow in borehole systems [38]. They observed that the property of the rock in different regions is similar but that the values of thermal conductivity and thermal resistance are different. They also mentioned that improvements in the thermal capacities of boreholes can be explained by the occurrence of groundwater flow in the rock and natural convection in the system [38].

Florides et al. (2011) discussed the analysis of heat flow through a borehole heat exchanger. They developed and validated a numerical model for the simulation of energy and temperature change in a U-tube model. Software (FlexPDE) was employed to solve the resulting boundary values [39]. They formulated a mathematical model for geothermal heat exchangers. The model was used to formulate the heat transferred from the fluid to each of the legs of the geothermal heat exchanger and through them to the borehole and soil material. Two real-life cases were set up and the material thermal properties were compared with the experimental results to see that they fitted the typical values. Fig. 2.16 shows a 3D image of the employed mesh [39].

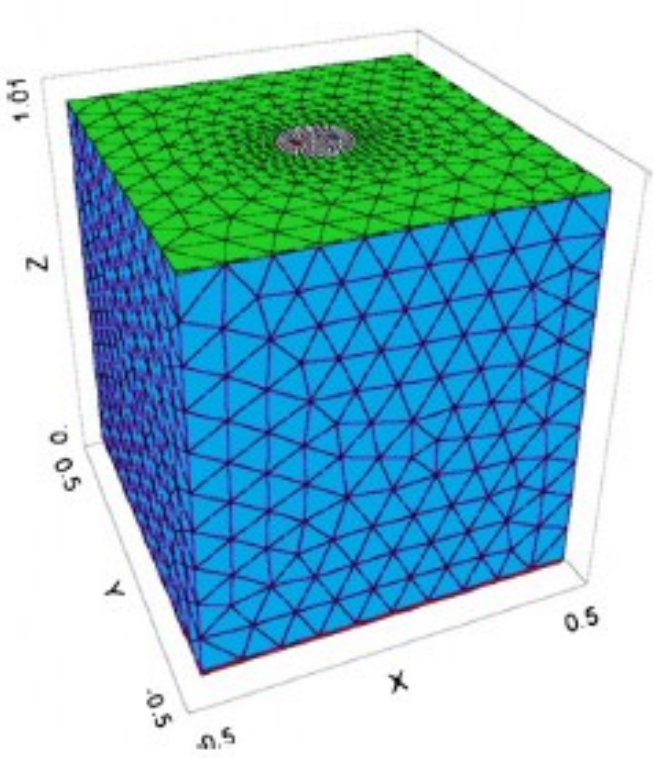

Figure2.16: 3D image of the resulting mesh [39]

Eslami-nejad and Bernier (2011) discussed the coupling of geothermal heat pumps with thermal solar collectors using double U-tube boreholes with two independent circuits. They presented a model which predicts the fluid temperature in two independent circuits. The U-tube borehole model configuration was studied, with one circuit linked to a ground-source heat pump and the other to thermal solar collectors. All systems were simulated for 20 years for a residential-type single borehole configuration. It was also shown that the impact on annual heat pump energy consumption was less dramatic, with corresponding reductions [40].

Mendez et al. (2010) discussed the evaluation of the multiple transport model MT3DMS for heat transport simulation of closed geothermal systems. They suggested that MT3DMS should be able to simulate heat transport if buoyancy and viscosity changes are minimal. They evaluated the simulations of GSHP through two approaches, and they found that MT3DMS can be successfully applied to simulate GSHP systems. Also, other systems with similar temperature ranges and gradients in saturated porous media can be evaluated [41].

Li et al. (2006) provided numerical and experimental simulations on the thermal performance of a U-vertical ground-coupled heat exchanger (UGCHE). Single season and double season operations were performed. The temperature contours are shown in Fig. 2.17 [42]. They stated that the experiments show that the ground source can be used as the heat source/sink for GCHP systems in order to have higher efficiency in saving energy [42].

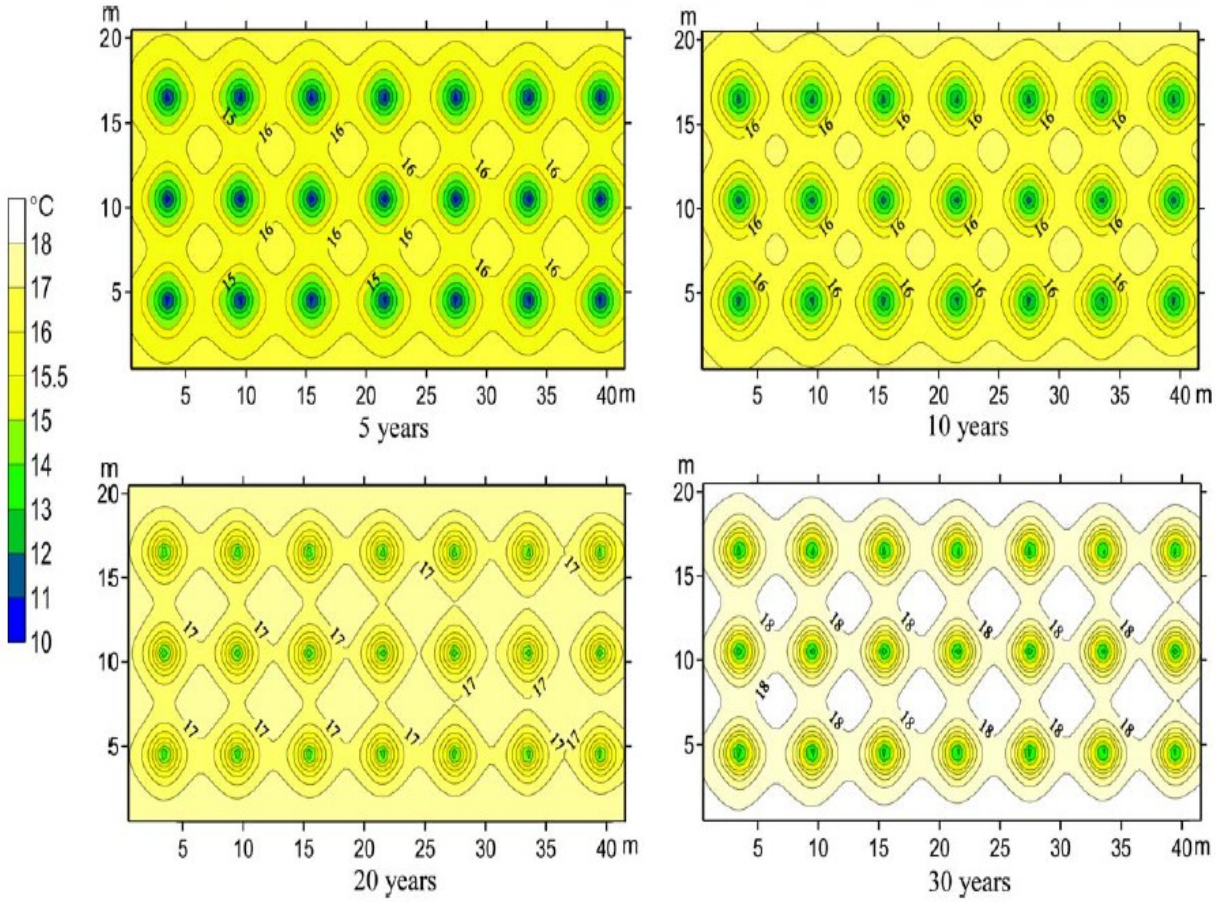

Figure2.17: Temperature contours after 5, 10, 20, and 30 years [42]

Choi et al. (2011) discussed the numerical simulation of vertical ground heat exchangers for unsaturated soil conditions. They simulated the effect of varying the thermal properties of inhomogeneous unsaturated soil on the intermittent operation of a vertical GHE. A three-phase soil model was used to introduce soil properties that vary with depth. They observed that the performance of the system during the first few hours was significantly different from the analytical infinite line source model. They also concluded that the unsaturated soil conditions afford a lower mean heat exchange rate then saturated

conditions. Fig. 2.18 demonstrates the top view image of the three-dimensional finite element models [43].

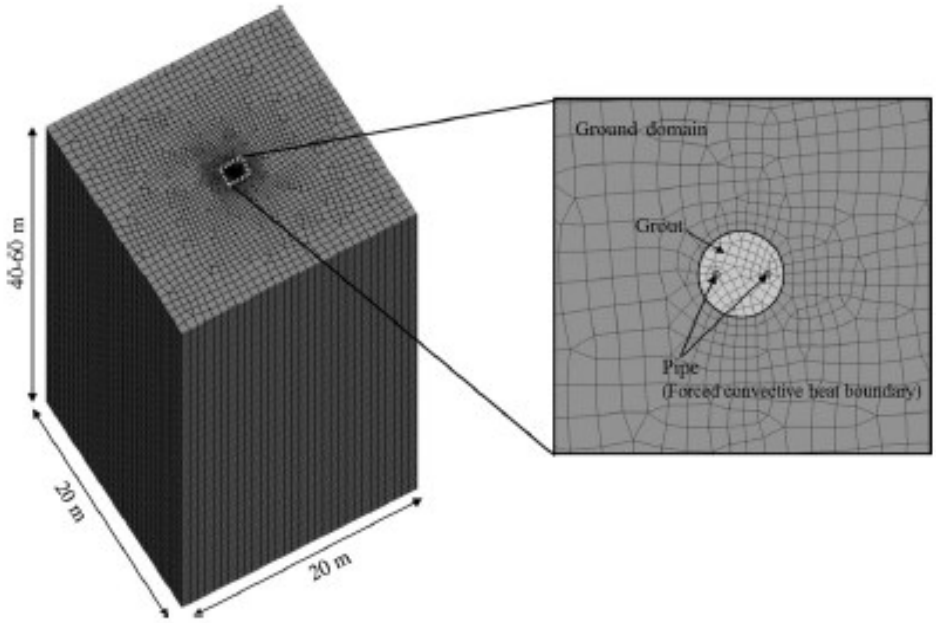

Figure 2.18: 3-D finite element model top view [43]

In summary, various aspects of shallow geothermal systems have been extensively studied, and numerical methods based on heat conduction equations have been widely used for the study of such systems. This motivates the use of the same equations for

studying deep geothermal systems, which have rarely been studied, as explained in the next chapter.

Chapter 3: A modified design for deep geothermal systems and numerical modeling

This chapter discusses about a new design[1] for deep geothermal energy systems and will also present a numerical model and its parameters.

The basic aim of the project is to generate 2 MW of electricity. The system includes a main well and several side channels at an angle (40^0) to the main well so that heat can be absorbed by the side channels and the main well. Heat pipes are installed to absorb and transport thermal energy to the surface.

In the first step, the total drilling length of the system is maintained to be a constant 10,000m by varying the other parameters, such as the depth of the side channel and the main well. Fig. 3.1 shows a schematic view of the system design including the side channels, main well, and ORC. The power collected is converted into electricity by implying ORCs or turbines.

[1] Developed by Cubit Power Systems

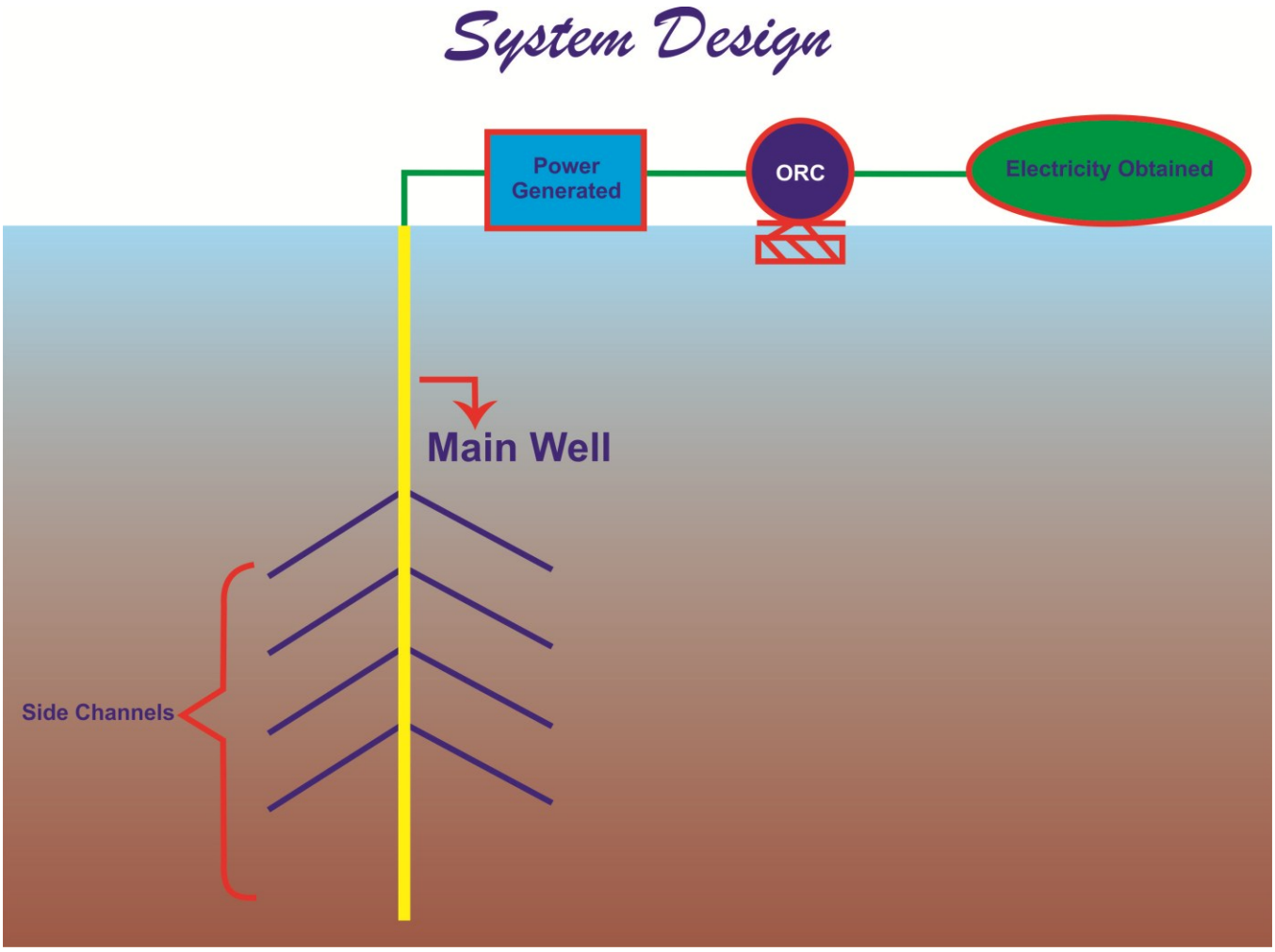

Figure3.1: Flowchart showing the system model

In this following, the numerical model used in the calculations is briefly reviewed.

3.1. Governing equation

The governing equation is the heat conduction equation given by

$$\frac{\partial T}{\partial t} = K_x \frac{\partial^2 T}{\partial x^2} + K_y \frac{\partial^2 T}{\partial y^2} + K_z \frac{\partial^2 T}{\partial z^2} + S \qquad (3.1)$$

where K_x, K_y, and K_z are, respectively, the thermal diffusion coefficient in the *x*, *y*, and *z* directions, *T* is the temperature, *t* is the time, and S is the heat source or sink. In the present research, the term *S* represents the heat absorbed by the heat pipe. In this research, isotropic homogeneous conditions were assumed. That is,

$$K_x = K_y = K_z = K \tag{3.2}$$

The equation (3.1) only considers the heat transport due to conduction. Since one is dealing with deep geothermal systems, the advection term due to the movement of ground water is assumed to be negligible and is not considered in the equations.

3.2. Numerical scheme

The three-dimensional heat transport (diffusion) equation is solved by a finite difference method based on the heat flux using a variable grid size. The discretized form of the first term (temporal variation) is given by

$$\frac{\partial T}{\partial t} = \frac{T_{i,j,k}^{n+1} - T_{i,j,k}^{n}}{\Delta t} \tag{3.3}$$

where Δt is the time step size, chosen to be constant in this project, and $T_{i,j,k}^{n}$ and $T_{i,j,k}^{n+1}$ are, respectively, the temperature at times $t = n\Delta t$ and $t = (n+1)\Delta t$ at the location represented by the grid point *(i,j,k).*

The spatial derivatives are discretized using a second-order centered difference scheme over a variable grid size, as

$$\frac{\partial^2 T}{\partial x^2} = \frac{\left(\frac{\partial T}{\partial x}\right)_{i+\frac{1}{2},j,k} - \left(\frac{\partial T}{\partial x}\right)_{i-\frac{1}{2},j,k}}{x_{i+\frac{1}{2},j,k} - x_{i-\frac{1}{2},j,k}} = \frac{\left(\frac{T_{i+1,j,k} - T_{i,j,k}}{x_{i+1,j,k} - x_{i,j,k}}\right) - \left(\frac{T_{i,j,k} - T_{i,j-1,k}}{x_{i,j,k} - x_{i,j-1,k}}\right)}{x_{i+\frac{1}{2},j,k} - x_{i-\frac{1}{2},j,k}} \tag{3.4}$$

$$\frac{\partial^2 T}{\partial y^2} = \frac{\left(\frac{\partial T}{\partial y}\right)_{i,j+\frac{1}{2},k} - \left(\frac{\partial T}{\partial y}\right)_{i,j-\frac{1}{2},k}}{y_{i+\frac{1}{2},j,k} - y_{i-\frac{1}{2},j,k}} = \frac{\left(\frac{T_{i,j+1,k} - T_{i,j,k}}{y_{i,j+1,k} - y_{i,j,k}}\right) - \left(\frac{T_{i,j,k} - T_{i,j,k-1}}{y_{i,j,k} - y_{i,j,k-1}}\right)}{y_{i+\frac{1}{2},j,k} - y_{i-\frac{1}{2},j,k}} \tag{3.5}$$

$$\frac{\partial^2 T}{\partial z^2} = \frac{\left(\frac{\partial T}{\partial z}\right)_{i,j,k+\frac{1}{2}} - \left(\frac{\partial T}{\partial z}\right)_{i,j,k-\frac{1}{2}}}{z_{i,j,k+\frac{1}{2}} - z_{i,j,k-\frac{1}{2}}} = \frac{\left(\frac{T_{i,j,k+1} - T_{i,j,k}}{z_{i,j,k+1} - z_{i,j,k}}\right) - \left(\frac{T_{i,j,k} - T_{i,j,k-1}}{z_{i,j,k} - z_{i,j,k-1}}\right)}{z_{i,j,k+\frac{1}{2}} - z_{i,j,k-\frac{1}{2}}} \tag{3.6}$$

Finally, the complete discretized system is written as

$$\frac{T_{i,j,k}^{n+1}-T_{i,j,k}^{n}}{\Delta t}=\frac{\left(\frac{T^{n}{}_{i+1,j,k}-T^{n}{}_{i,j,k}}{x_{i+1,j,k}-x_{i,j,k}}\right)-\left(\frac{T^{n}{}_{i,j,k}-T^{n}{}_{i,j-1,k}}{x_{i,j,k}-x_{i,j-1,k}}\right)}{x_{i+\frac{1}{2},j,k}-x_{i-\frac{1}{2},j,k}}+\frac{\left(\frac{T^{n}{}_{i,j+1,k}-T^{n}{}_{i,j,k}}{y_{i,j+1,k}-y_{i,j,k}}\right)-\left(\frac{T^{n}{}_{i,j,k}-T^{n}{}_{i,j,k-1}}{y_{i,j,k}-y_{i,j,k-1}}\right)}{y_{i+\frac{1}{2},j,k}-y_{i-\frac{1}{2},j,k}}+\frac{\left(\frac{T^{n}{}_{i,j,k+1}-T^{n}{}_{i,j,k}}{z_{i,j,k+1}-z_{i,j,k}}\right)-\left(\frac{T^{n}{}_{i,j,k}-T^{n}{}_{i,j,k-1}}{z_{i,j,k}-z_{i,j,k-1}}\right)}{z_{i,j,k+\frac{1}{2}}-z_{i,j,k-\frac{1}{2}}}+S_{i,j,k}^{n} \tag{3.7}$$

The above numerical method is first-order in time and second-order in space. It is very efficient because the discretization is explicit and therefore there is no need to solve a linear system of simultaneous equations. Other numerical methods such as an implicit finite difference method and an ADI scheme with second-order accuracy in time were also considered, but it was found that the computational cost is not justified by the gain in accuracy and so it would be better to use the first-order scheme but using a finer computational grid. The overall computational cost of this approach was found to be lower than employing a more accurate numerical method with a coarser grid.

On the other hand, a fine numerical grid is needed anyway for modeling the impact of heat pipes on the system. Finally, the temporal changes are very small because the process is very slow (typically of an order of years), and therefore a large time step size would be also accurate. Indeed, through numerical experiments, one found that the step

size is more controlled by stability than accuracy. Stability of a numerical method deals with its ability to suppress small numerical errors caused by truncation errors or round-off errors, and implicit methods are typically more stable. That is, numerical errors do not accumulate in those schemes. However, implicit schemes are computationally more expensive due to the need to solve a linear system of simultaneous equations, and as mentioned before, one can find that an explicit method is more efficient for the present research.

3.3. Calculation of the source term

Temperature is absorbed by the heat pipe. The amount of the absorbed thermal energy is controlled by the rate of flow inside the heat pipe. Let one assume that the amount of energy extracted from a computational cell of size $\Delta v = \Delta x \times \Delta y \times \Delta z$ over time Δt is equal to ΔE. Then, the change of temperature in the computational cell caused by the extraction of energy may be calculated as

$$\Delta T = \frac{\Delta E}{\rho \Delta v C} \tag{3.8}$$

where C represents specific heat capacity ($J^oC^{-1}kg^{-1}$) and ρ is the density (kg/m^3). The source term S is then calculated as

$$S = \frac{\Delta T}{\Delta t} \tag{3.9}$$

Therefore,

$$S = \frac{\Delta E}{\rho \Delta v C \Delta t} \tag{3.10}$$

In the numerical simulations, the total extracted energy is projected based on the demand curve and is uniformly divided among the computational cells that include the heat pipe. The source term is then calculated from the equation (3.10) for those cells and is set as equal to zero for other computational cells. The presence of the source term in some computational cells leads to a heat flow towards those cells.

3.4. Computer program

Numerical simulations are conducted using a computer program written in FORTRAN language using the INTEL FORTRAN compiler. The program uses the OPENMP parallel library for parallel processing, which considerably reduces the computational cost. The computations were performed on a server with 24 processors, and simulation time was typically between 16 to 72 hours depending on the thermal diffusivity coefficient and computational grid.

3.5. Computational grid and boundary conditions

Due to the symmetry of the system, only a quarter of the system was simulated, and the resulting power was multiplied by four. As mentioned before, a variable-size structured grid is used. The grid size is fine around the heat pipes where energy is extracted, and gradually becomes coarser far from those locations. The grid independency and time step independency analyses are also performed in order to make sure the grid size and time step are small enough. In most simulations, a large number of up to 100,000,000 grid

points were employed. A typical slice of the grid from a top view is shown in Figure 3.2. The dark sections in the figure represent the sections where the mesh is too fine to be well illustrated, and those sections are where it is important to have more precision. The boundary conditions are constant temperature at all boundaries, and symmetry at the center. The boundaries are located far enough from the pipes so that the assumption of constant temperature remains valid.

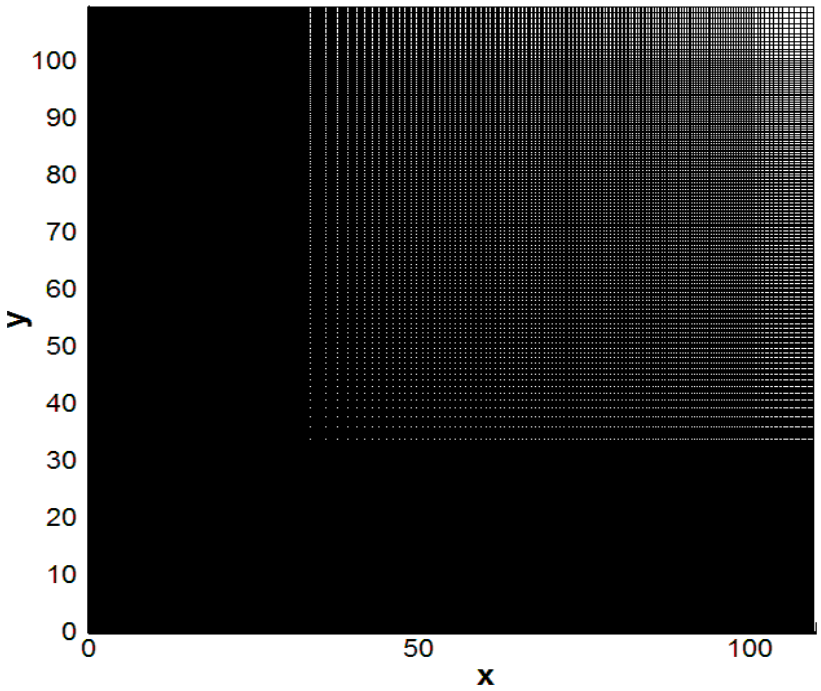

Figure3.2: X-Y view of a mesh

A typical simulation result is shown in Figure 3.3 (a vertical slice of the three-dimensional grid). Colours show the temperature based on the legend presented in the same figure. The heat pipes are identified by the light blue colour. As can be seen in this

figure, the temperature drops around the heat pipes and affects the total temperature field in the system.

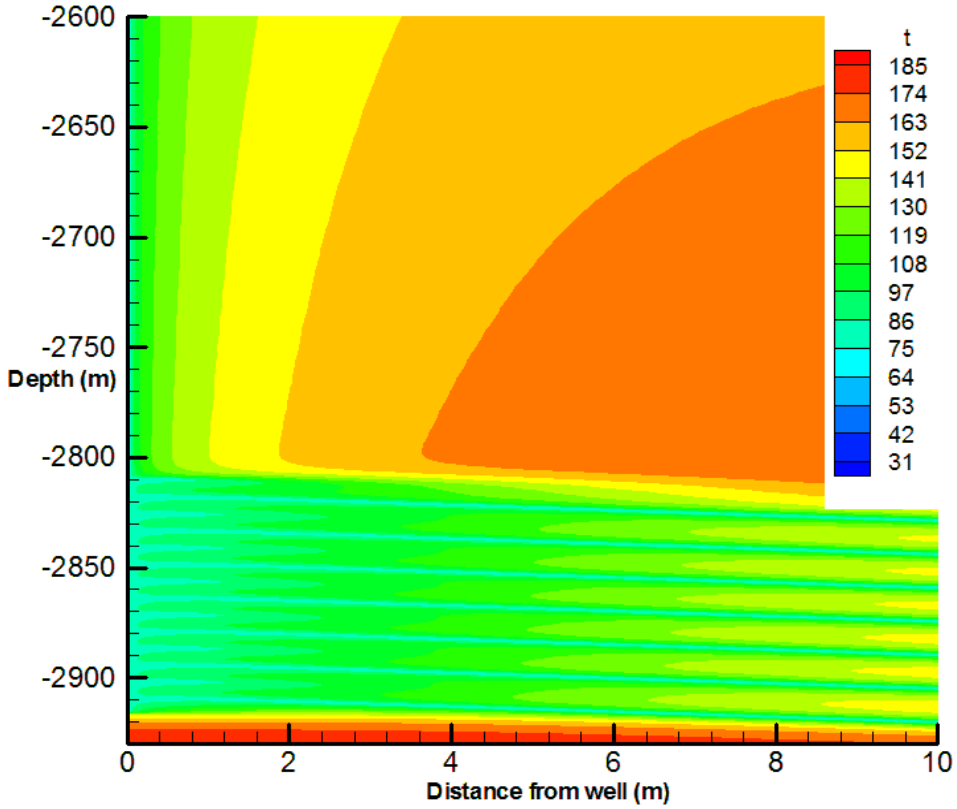

Figure3.3: Typical simulation result where colours show the temperature difference. Heat pipes are identified by the light blue colour.

3.6. Typical output power

In this project, the performance of a geothermal power plant is analysed based on the power generated with respect to time. A typical plot of the output power generated with respect to time for a typical geothermal power plant is shown is Fig. 3.4. From the figure, we can observe that the power generation rate is initially much higher than the

required 2 MW and has a drastic drop with respect to time after the initial days of operation. Such a steep/sudden decrease in the power generation after the initial few days indicates that the system is stable for only a certain period. This will certainly dent the performance of the system. Moreover, the power generated does not reach a steady state condition and keeps decreasing as time increases in this case.

Our goal is to generate power according to a demand curve with an optimal condition of 2 MW in order to obtain an economical and optimal system. Using the valves installed on the heat pipes, one can control the amount of the extracted heat. One can therefore maintain the generation rate close to the required amount (2 MW) for a longer period of time and increase the sustainability of the system. An economic analysis is performed in Chapter 4 to determine the feasibility of the system under various conditions with respect to the demand curve. The system lifetime obtained from the financial analysis would be considered as a target for determining the system performance.

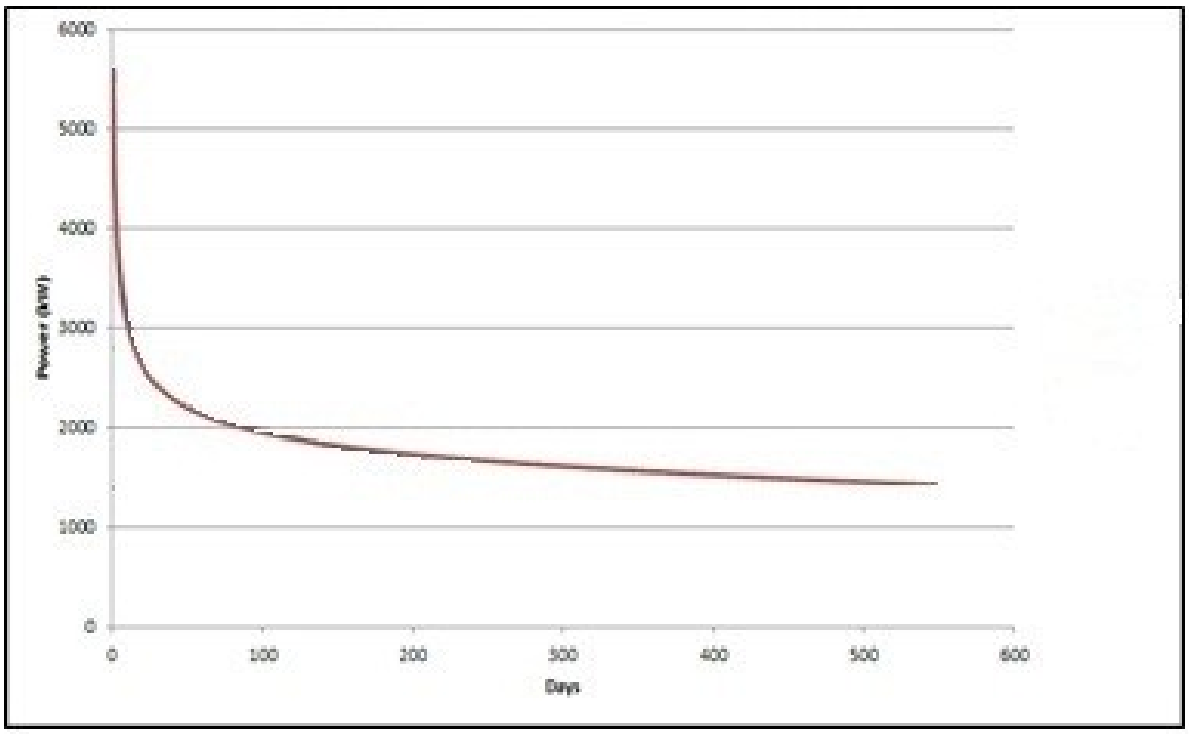

Figure3.4: Typical output power versus time (days)

3.7. Demand curve

As mentioned previously, the major aim of this project is to develop an optimal geothermal energy system which generates maximum power. A typical demand curve has been used[2], as shown in Fig. 3.5.

The demand curve has a sinusoidal pattern of increasing and decreasing function. As shown in Fig. 3.5, the demand energy increases each day in the evening and decreases in

[2] Provided by Cubit Power Systems

the morning. This periodic form is followed in the numerical model in order to simulate operational conditions which help in increasing the life time of the system.

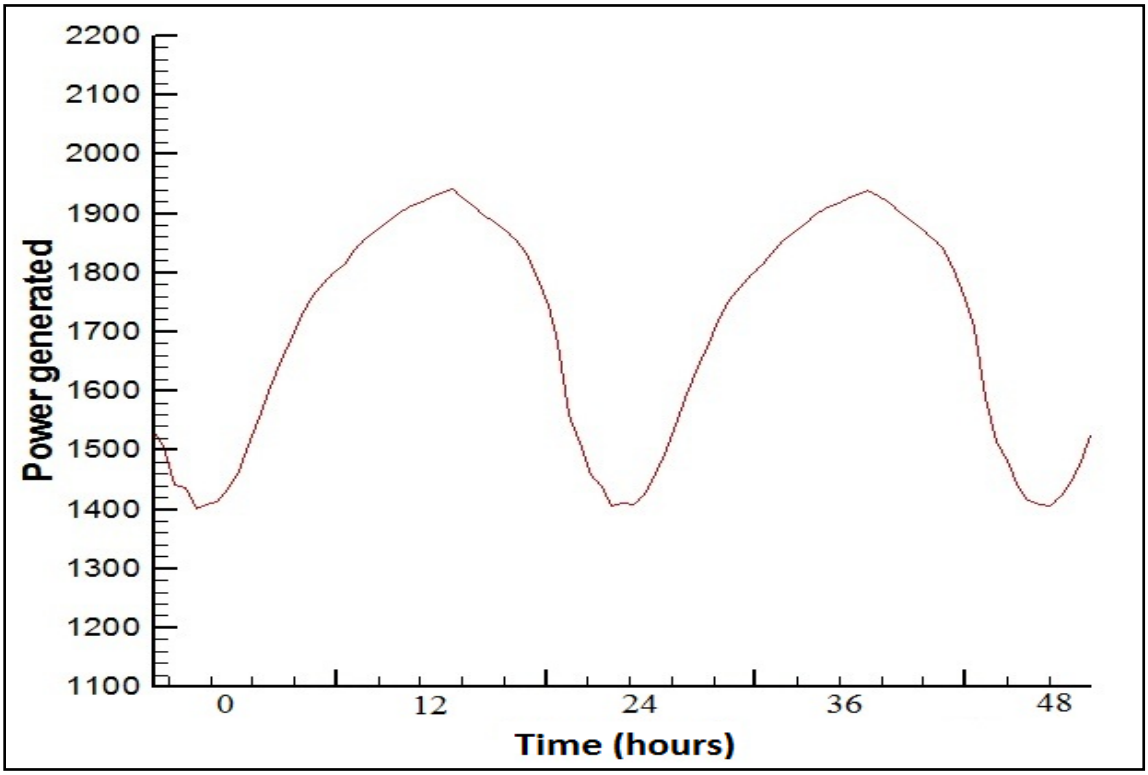

Figure3.5: Demand curve performance

The performance of the simulation is always monitored in order to check if the system is following the demand curve, and if not, the required changes are made to the input file. The results obtained from these simulations were viewed using 'Tecplot", which

gives a 2-D image/plot of the results. Typical result performance is shown in Figures 3.6 and 3.7.

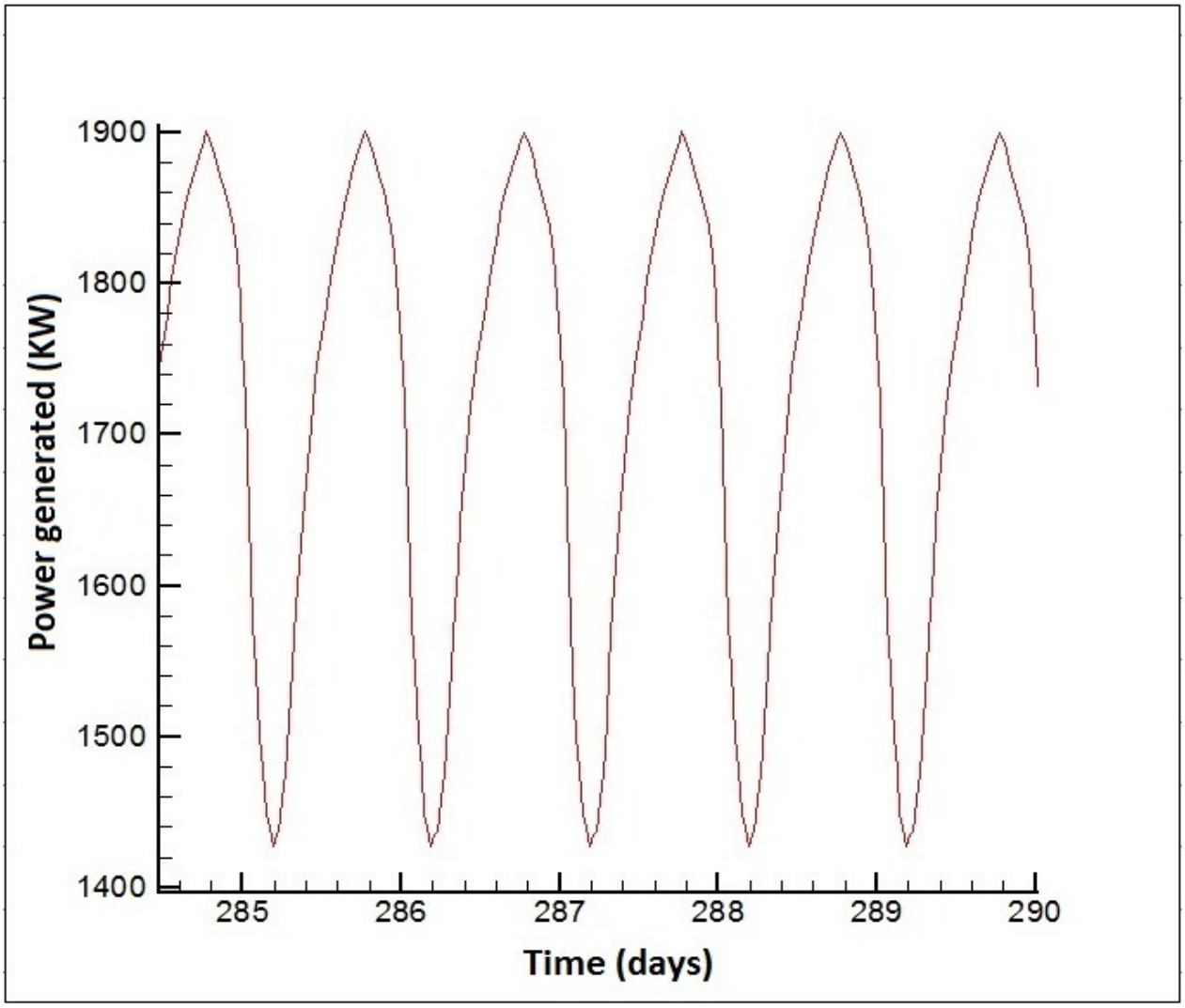

Figure3.6: Sinusoidal performance of the system.

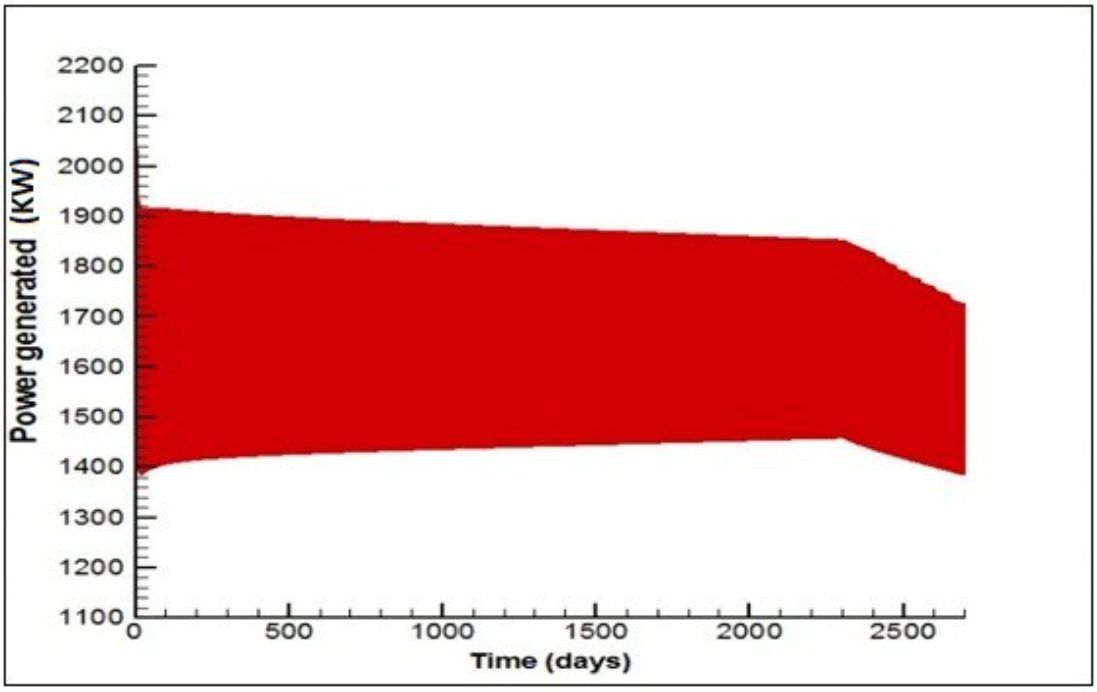

Figure3.7: 2D image of the simulation

Fig. 3.7 shows the performance of the simulation, where it is observed that the power generated is maintained between 1400 KW and 1900 KW, and the time in days is about 2300. We can also observe that there is a sudden decrease in the power generated after this point (2300 days) which determines the lifetime of the system; i.e. under the given conditions the system is stable up to a certain time and can generate the required power, but after this time, power generation starts to decrease quickly.

As a summary, one can state that chapter 3 gives information about the numerical model and system design. The typical performance of a geothermal energy system is shown and also talks about the demand curve and its performance.

Chapter 4: Financial analysis

In this chapter the analysis of the cost required for the system based on the total drilling length, drilling cost, maintenance cost, electricity price, etc. is performed. The total cost is calculated based on the individual costs of each parameter and is compared to see if the system is economical or not.

4.1. Budgeting

Budgeting is one of the primary tasks while starting any project. It gives a start-off financial view of the project and allows one to estimate the financial value of the project. All the costs and expenses that will be incurred throughout the project are estimated during budgeting. So, it allows one to decide on the magnitude of a project and also gives a sense of the feasibility of the project in terms of financial resources.

The extent of the project and the amount of resources available can be matched against each other through this process. By this, one can have a primary view of all the potentially includable processes. Through budgeting, the affordability of the participating organization or individual can be measured, and thus it helps them to plan for the type of materials that should be used in the project and the amount that is affordable for them. A

very primary estimation of the feasible duration period of the project can also be determined.

4.2. Need for budgeting

The budget gives a picture of the time the project might need as well as the resources and materials necessary. Hence, the project can make use of this estimation and can progress based on it. Budgeting allows an individual or an organization to prepare a quotation for the whole project which can be used to depict the financial value of the project. Finally, budgeting is considered one of the most important primary tasks because it allows for an accurate prioritization in the allocation of available financial resources in order to suit the corresponding objectives of the project.

4.3. Budgeting for the geothermal power plant

Budgeting for the geothermal project gives an idea about the amount of initial investment required, which includes the cost of equipment, cost of maintenance, cost of raw material required, interest rates, inflation rates, etc. It also gives an idea about the financial value of the project and an approximate time as to when the returns can be obtained.

As one knows that setting up a geothermal power plant requires a lot of money as well as man- and mechanical power, the budgeting is a very important step. The major goal while designing a power plant is to have the best and the most economical design. Considering all the above parameters, the budgeting for the power plant has been done. The parameters used for the analysis are given below in Table 4.1.

Table4.1: System components and their costs

S. No.	Equipment	Cost	Reference
1.	Drilling	$ 365 per meter	Calling companies
2.	ORC with installation	$100,000	Cubit
3.	Heat pipe	$18.23 per meter	Calling companies
4.	Grout material	$7.32 per meter	Calling companies
5.	Electricity price	20 cents	CPI
6.	Interest rate	0.5 % per month	Cubit
7.	Inflation rate	0.0013 per month	CPI
8.	Inflation rate for electricity	0.00083 per month	CPI
9.	Maintenance cost	$5,500per month	Cubit

With respect to all the above parameters, the initial cost was calculated. As a deep geothermal system is considered, the total drilling lengths of the system are considered as 8,000m (26246 feet) and 10,000m (32,808 feet).

Calculations for a total drilling length of 8,000 m:

1. Cost of drilling = 365 [$/m] × 8000 [m] = $ 2920000.
2. Cost of heat pipes = 18.23 [$/m] × 8000 [m] = $ 145,840
3. Cost of grout material = 7.32 [$/m] × 8000 [m] = $ 58,560
4. Cost of ORC with installation = $100,000

By adding up all the above costs, the capital turns out to be approximately $3,300,000.

Calculations for a total drilling length of 10,000m:

1. Cost of drilling = 365 [$/m] × 10000 [m] = $ 3650000.
2. Cost of heat pipes = 18.23 [$/m] × 10000 [m] = $ 182,300
3. Cost of grout material = 7.32 [$/m] × 10000 [m] = $ 73,200
4. Cost of ORC with installation = $100,000

By adding up all the above costs, the capital turns out to be approximately $4,300,000. The calculations for the cost analysis are done for 300 months; i.e. 25 years. The sample calculations for the first year are shown in Table 4.2 below, and the rest were done in an Excel file.

Based on the demand curve for the system, the power generation rate is expected to vary between 2000 KWH and 1400 KWH. Hence, an average value of 1700 KWH is considered for cost-benefit calculations. Fig. 4.1 shows the expected average power generation with respect to the system lifetime, used in financial analysis. A straight line is seen, as a constant power generation rate has been considered.

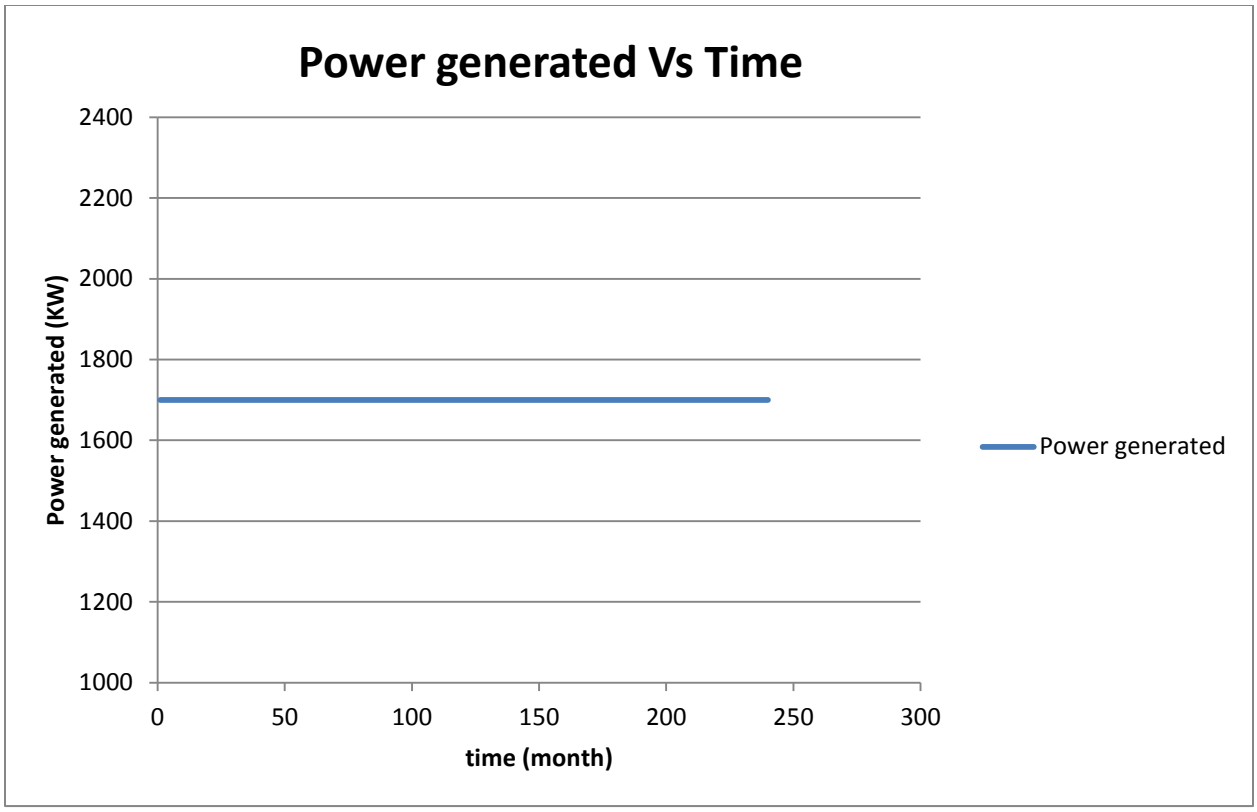

Figure4.1: Expected average power generation with respect to time (months)

4.4. Calculations for cost analysis

4.4.1. Total drilling length 8,000m

With the parameters in Table 4.1, the cost analysis calculation for a total drilling length of 8,000m is performed on an Excel sheet, and Table 4.2 shows the results for the first 12 months.

Table 4.2: Cost analysis for a total drilling length of 8000m

Month	Power (KW)	Electricity	Cost	Income	Total cost
1	1,700	0.2	-3500000	36720	-3463280
2	1,700	0.200166	-5500	36750.48	-3449346
3	1,700	0.2003321	-5507.15	36780.99	-3435319
4	1,700	0.2004984	-5514.31	36811.51	-3421198
5	1,700	0.2006648	-5521.48	36842.07	-3406984
6	1,700	0.2008314	-5528.66	36872.64	-3392675
7	1,700	0.2009981	-5535.84	36903.25	-3378271
8	1,700	0.2011649	-5543.04	36933.88	-3363771
9	1,700	0.2013319	-5550.25	36964.53	-3349176
10	1,700	0.201499	-5557.46	36995.21	-3334484
11	1,700	0.2016662	-5564.69	37025.92	-3319695
12	1,700	0.2018336	-5571.92	37056.65	-3304809

Sample calculations are presented in the following. Note that an efficiency coefficient of 0.15 is considered for the conversion of thermal energy to electrical energy. All sample calculations are performed on the basis of the 2nd month:

- **Cost of electricity** = Initial cost of electricity * (1+IR for electricity)

  = 0.20 * (1+0.00083) = **0.2001**

- **Cost of maintenance** = Maintenance cost * (1+Inflation rate)

  = 5500 * (1+0.0013) = **-5507.12**

- **Income** = Power generated * electricity price

  = 1,700 * 0.2001 * 24 hrs * 30 days*0.15

  = 36750.48

- **Total Cost** = Cost of maintenance + Income + Total cost of previous month * (1+ interest rate per month)

  = (-5500) + (36,750.48) + [(-3463280)* (1+0.005)]

  = -3449346

Based on the calculation and the numbers obtained, one can plot a graph with respect to 'total cost versus time'. Fig. 4.2 shows the graph for total costs with respect to time.

4.4.2. Total drilling length 10000m

With the parameters in Table 4.1, the cost analysis calculation for a total drilling length of 10000m is performed on an Excel sheet, and Table 4.3 shows the numbers for the first 12 months.

Table4.3: Cost analysis for a total drilling length of 10000m

Month	Power (KW)	Electricity	Cost	Income	Total cost
1	1700	0.2	-4300000	36720	-4263280
2	1700	0.200166	-5500	36750.48	-4253346
3	1700	0.2003321	-5507.15	36780.99	-4243339
4	1700	0.2004984	-5514.31	36811.51	-4233258
5	1700	0.2006648	-5521.48	36842.07	-4223104
6	1700	0.2008314	-5528.66	36872.64	-4212876
7	1700	0.2009981	-5535.84	36903.25	-4202573
8	1700	0.2011649	-5543.04	36933.88	-4192195
9	1700	0.2013319	-5550.25	36964.53	-4181741
10	1700	0.201499	-5557.46	36995.21	-4171212
11	1700	0.2016662	-5564.69	37025.92	-4160607
12	1700	0.2018336	-5571.92	37056.65	-4149925

Sample calculations for a total drilling length of 10,000m are presented in the following. Note that an efficiency coefficient of 0.15 is considered for the conversion of thermal energy to electrical energy.

All sample calculations are performed on the basis of the 2nd month:

- **Cost of electricity** = Initial cost of electricity * (1+IR for electricity)

  = 0.20 * (1+0.00083) = **0.2001**

- **Cost of maintenance** = Maintenance cost * (1+Inflation rate)

  = 5,500 * (1+0.008) = **-5507.15**

- **Income** = Power generated * electricity price

  = 1,700 * 0.2001 * 24 hrs * 30 days*0.15

  = 36,750.48

- **Total Cost** = Cost of maintenance + Income + Total cost of previous month * (1+ interest rate per month)

  = (-5,500) + (36,750.48) + [(-4,263,280)* (1+0.005)]

  = -4253346

Based on the calculations and the results obtained, a graph has been plotted with respect to 'total cost versus time'. Fig. 4.3 shows the graph for total costs with respect to time.

The calculations for present value analysis are also performed which is shown in Appendix II.

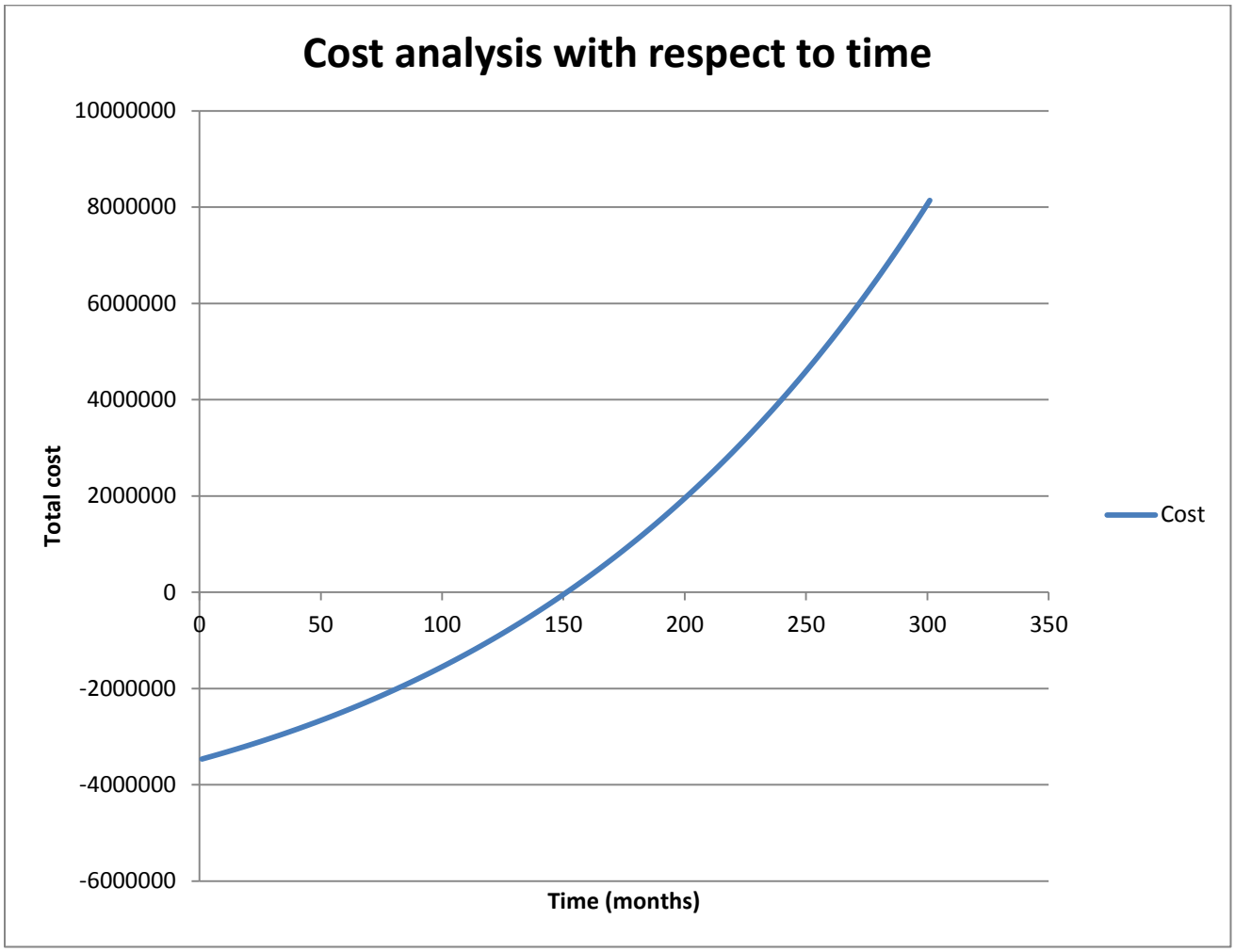

Figure4.2: Total cost versus time (months) for a total drilling length of 8,000m

Figure4.3: Total cost versus time (months) for a total drilling length of 10,000m

From Figures 4.2 and 4.3, one can observe that the break-even point for a total drilling length of 8,000 m is after 150 months (approximately 12 years), and for a total

drilling length of 10,000m it is after approximately 205 months (17 years). This shows that profit/returns can be expected for 8,000m and 10,000m total drilling lengths after 12 and 17 years respectively. On performing each simulation, one can analyse the performance of the system based on the financial report and thus obtain the best and the most economically feasible conditions.

Another major point which one can look for in such an analysis is the initial capital cost, which can go as high as $5.5 million, depending of the type of soil that will be used, the area of the land required, the ORC cost, and other parameters. Therefore, the feasibility of the project should be studied on a case by case basis.

Chapter 5: Sensitivity analysis and numerical results

In this chapter, the sensitivity of different parameters in the model is discussed, and the simulation results are presented for each condition.

5.1. Model Parameters

As mentioned earlier, the output power generated is calculated based on varying parameters, such as thermal diffusivity of the rock, depth of the main well, number of side channels, and also, the length of those side channels. All these different parameters have a major impact on the system design based on their influence on the output power. In the second stage of simulations, the total drilling length of the system is varied from 6,000m to 10,000m.

Important system parameters include:

a. Temperature gradient
b. Thermal diffusivity
c. Number and length of side channels

d. Distance between channels

e. Depth of main well

The performance of the design is tested by performing computer simulations using numerical code written in FORTRAN with the help of the Open MP library. Preliminary simulations were run in order to obtain typical characteristics of the system in accordance to the demand curve before performing the actual simulations. Using these typical parameters, one can subsequently look for optimal conditions for better power generation in every condition. The power generated is compared with respect to the total lifetime of the system in days. In this way, one can improve the lifetime of the system, as discussed below in the sensitivity analysis.

Table5.1: Range of Initial Parameters

Total drilling length (m)	**10,000**
Thermal diffusivity (mm^2/s)	0.6-1.5
Thermal conductivity (J/m3K)	1.5e6
No. of groups (8 channels per group)	7
Channel length (m)	125
Temperature Gradient ($^0C/m$)	0.035-0.065

Table 5.1 shows the range of parameters used to perform the simulations and the sensitivity analysis. In the next chapter, we proceed to the sensitivity analysis in order to determine the optimal design of the system for given parameters.

5.2. Sensitivity analysis

For obtaining the optimal conditions, a series of sensitivity analyses were performed for each of the required parameters.

5.2.1. Sensitivity to the grid size

One of the most important parts of the design is the size of the grid. Obviously it is preferred to have a small enough grid to have required accuracy, but it is also important not to have a very small grid, as it might increase the computational cost. Different grid sizes were used in order to determine the best grid with optimal conditions, and the final grid was obtained based on a sensitivity analysis. That is, the grid size was reduced until the generated power became insensitive to the grid size.

5.2.2. Sensitivity to the time step size

Firstly, a time step analysis was conducted to find the biggest time step that could be used to increase the simulation time without compromising on the precision, which is the amount of power generated.

The time step analysis is done with varying numbers, starting from 100s to 2000s. The reason to perform the time step analysis is to find out the time taken for each simulation to be as quick as possible without compromising the amount of power generated. In this way, one can actually perform more simulations in a shorter time span.

Ideally it is preferable to obtain the result with the optimal case of best time step and maximum output power. Also one does not want a situation where increasing the time step leads to inaccuracy in the capacity of the power generation system.

The time step size depends on the thermal diffusivity of the system; i.e. by decreasing the thermal diffusivity of the system, the time step can be improved and vice-versa. Using sensitivity analysis, it was found that at a thermal diffusivity of 1.5 mm^2/s one could obtain the best time step of 1800 s. It was also noticed that the change in power generation was minimal, which can be ignored when considered at a larger scale point. It should be mentioned that one can increase the time step when we perform simulations with lower diffusivities.

5.2.3. Sensitivity to the depth of main well

The next set of simulations for the sensitivity analysis were performed by varying the depth of the main well from 2,000 to 5,000m in order to find the best possible length. The system is designed in such a way that the heat is collected by the side channels from the deep levels and is transferred to the main well. Therefore, the best depth of the main well must be determined in order to maximize the lifetime of the system.

The deeper we go into the Earth's surface, the higher the temperature will be, which means that more heat will be available to the side channels. Another important factor is that it is economical to drill from the surface straight down as compared to drilling at an

angle. Determining the deepest possible depth without compromising on the power generated will help in minimising the drilling cost.

The results obtained through the analysis of the main well depth are presented in Table 5.2

Table5.2: Depth of main well

Depth (m)	Life time of the system (days)
2000	60
2500	625
2800	1250
3000	1650
4000	4150
4300	4800
4500	5350
5000	6500

From the results, one can see that the lifetime of the system is maximized for the depth of 5,000 m. Based on drilling limitations, the depth of the main well should not exceed 5,000m.

5.2.4. Sensitivity to the vertical distance between lateral channels

Since the basic idea of the design is to develop a model which generates more power while minimizing cost, as a part of analyzing the different parameters, the impact of the vertical distance between the channels could be significant. As it is observed that it is preferable to have a longer main well, the distance between the side channels becomes very important. This is because one does not want a system where the side channels are too close to each other, which leads to interaction between channels, or too far away, which might reduce the extracted heat due to moving to shallower depths.

On performing this analysis, the major goal would be to determine the optimal distance between channels. Moreover, it is preferable to have a fewer number of side channels with the required spacing. Multiple simulations were performed by considering different lengths of the side channels at different depths, and the optimal distance between the side channels was obtained for various conditions, as explained later in the numerical results.

5.2.5. Sensitivity to the number and length of side channels:

The other parameter which is a major factor is the number of side channels and the length of each channel. As mentioned earlier, it is preferable to have a fewer number of channels with longer length, as it is beneficial to the drilling cost of the system, but more importantly to make sure that maximum power is generated.

From the previous analyses of the depth of the main well and the vertical distance between side channels, it is easier to determine the optimal number and length of side channels. The combination of number and length of channels has to be measured based on the depth of the main well.

The length and the number of side channels have to be complimented with each other such that the total drilling length is restricted to a maximum of 10,000m. A set of sample calculations performed for the length and number of side channels with respect to the total drilling length is shown in Table 5.3. The length of the main well was maintained as a constant of 5,000m, obtained from Table 5.2.

Table5.3: Length and number of channels used in optimization for total drilling length of 10,000 m

Distance between side channels	Number of side channel groups	Depth of side channel (m)	Depth of main well (m)	System lifetime (days)
45	5	127.5	5,000	11,570
45	6	106.25	5,000	11,700
45	7	91.08	5,000	11,600
45	8	79.7	5,000	11,300

No. of channels per group = 8

Note that the total drilling length of the system is equal to the depth of the main well plus the total drilling length of side channels. From the numerical results, shown in Table 5.3, the optimal number of groups of side channels was found to be 6. The numerical experiments were repeated for other values of distance between side channels, and it was found that the optimal number of groups remained constant (6 groups). Therefore, in all computations presented below, the number of groups is set as equal to 6.

5.3. Numerical results

By considering all the different parameters and conditions analysed in the sensitivity analysis, a number of simulations were performed for different total drilling lengths of 10,000m and 8,000m. Approximately, about 120 simulations were performed and the time of each simulation was between 16hrs - 72 hrs.

The first analysis in the results is the depth of the main well. As mentioned previously, the simulations were performed by considering different depths, varying from 2,000-5,000m. Fig. 5.1 shows that at a depth of 5,000m, the lifetime of the system is about 6,500 days.

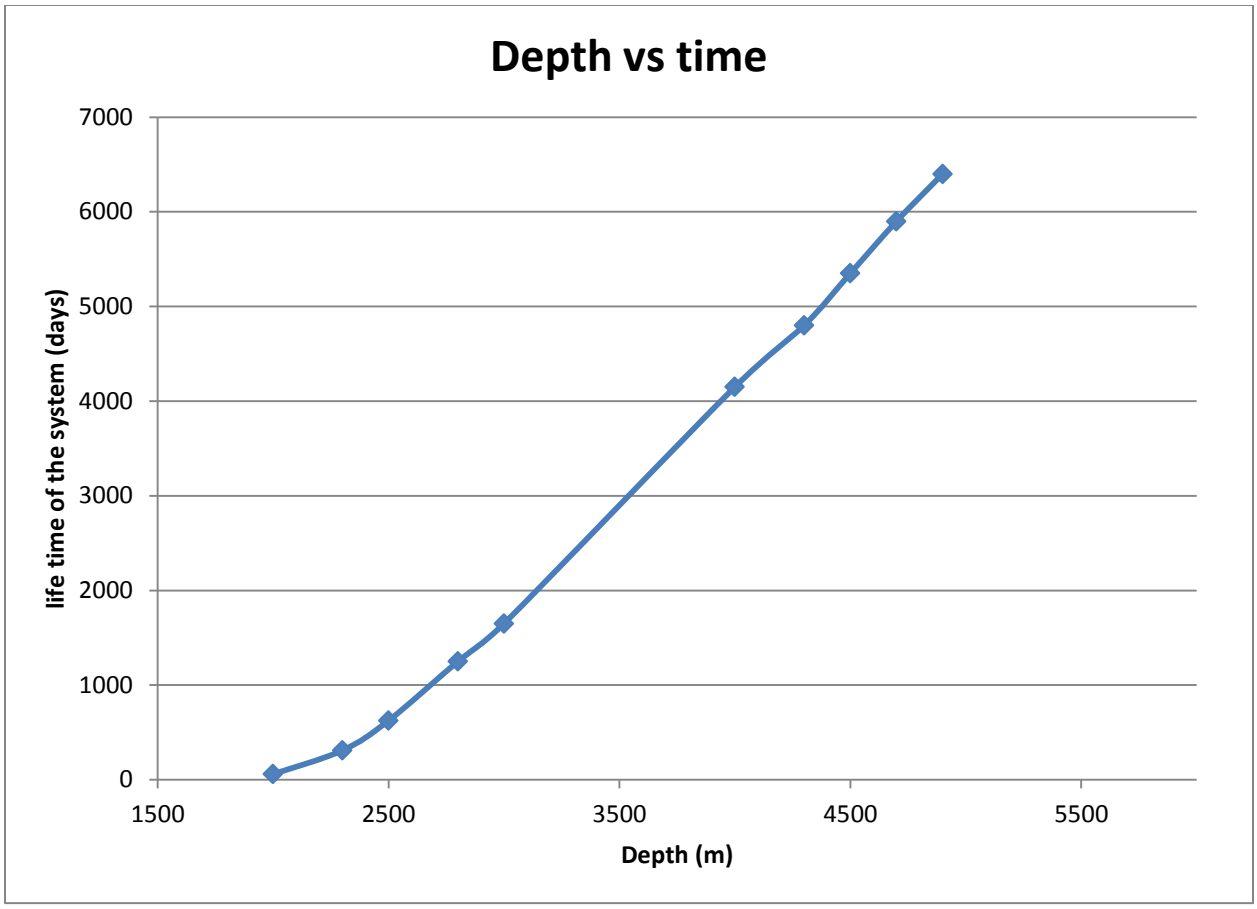

Figure5.1: Depth of main well vs. time

The second analysis is the distance between side channels with respect to the number of channel groups, as explained in the following.

From Fig. 5.1 it is observed that maximum power generation can be achieved at a vertical main well depth of 5,000m. Subsequently, the best distance between the side channels is obtained by considering the main well depth of 5,000m. The amount of power generated was adjusted according to the demand curve, and the resulting lifetime of the system in days was obtained with respect to the distance between side channels.

The thermal diffusivity coefficient is a major parameter controlling the lifetime of the system. To test the performance of the system and obtain the best design under various conditions, the simulations were performed with different diffusivities, which are discussed below.

5.3.1. Total drilling length of 10,000m

After obtaining the optimal depth of the main well and the number and length of side channels, now one can determine the lifetime of the system for a total drilling length of 10,000m with respect to various temperature gradients. All simulations are performed at three different thermal diffusivity coefficients, of 0.9 mm^2/s, 1.2 mm^2/s, and 1.5 mm^2/s.

The lifetime of the system versus the distance between the side channels at different temperature gradients of $35^0C/km$, $45^0C/km$, $55^0C/km$, and $65^0C/km$ is displayed in Figures 5.2 to 5.5.

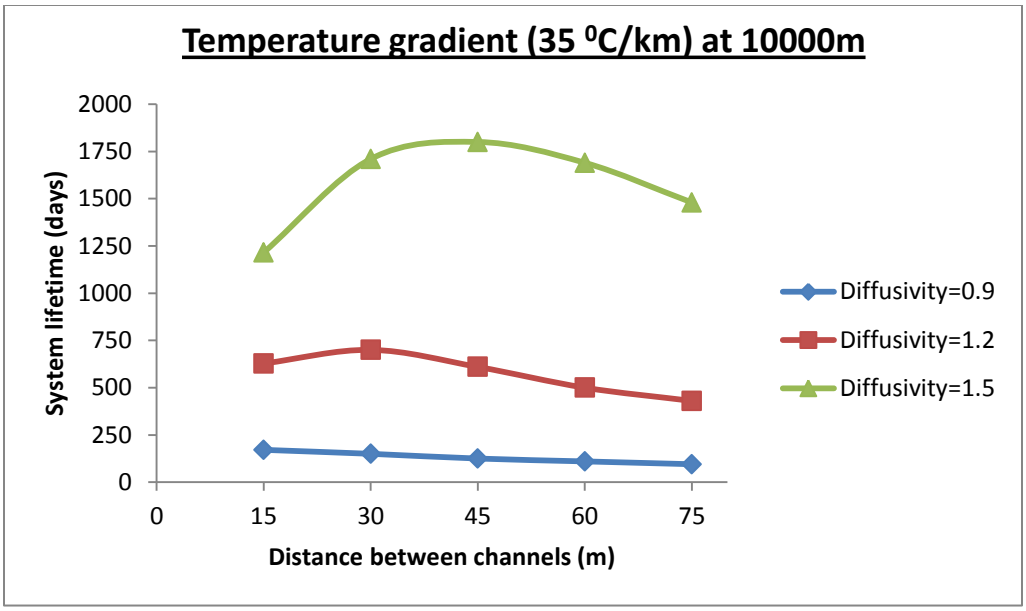

Figure5.2: System lifetime with respect to the distance between channels for a geothermal gradient of 35⁰C/km and a total drilling length of 10,000m

The performance of the system at a total drilling length of 10,000m and a temperature gradient of 35⁰C/km is shown in Figure 5.2. It can observed that the system lifetime is too short and does not reach the target of 17-year system lifetime and 2 MW power generation. The simulations are performed at three different thermal diffusivity values, of 0.9, 1.2, and 1.5 mm^2/s, and the target is not achieved in any of these three conditions.

The maximum lifetime of the system is achieved for the thermal diffusivity of 1.5 mm^2/s, as expected. The optimal distance between the side channels is around 40 m in this case. However, even in that case, the maximum lifetime of the system is only 1,800 days, which is far less than the required target. Therefore, one can conclude that the system is not economically feasible for locations with a geothermal gradient of 35⁰C/km.

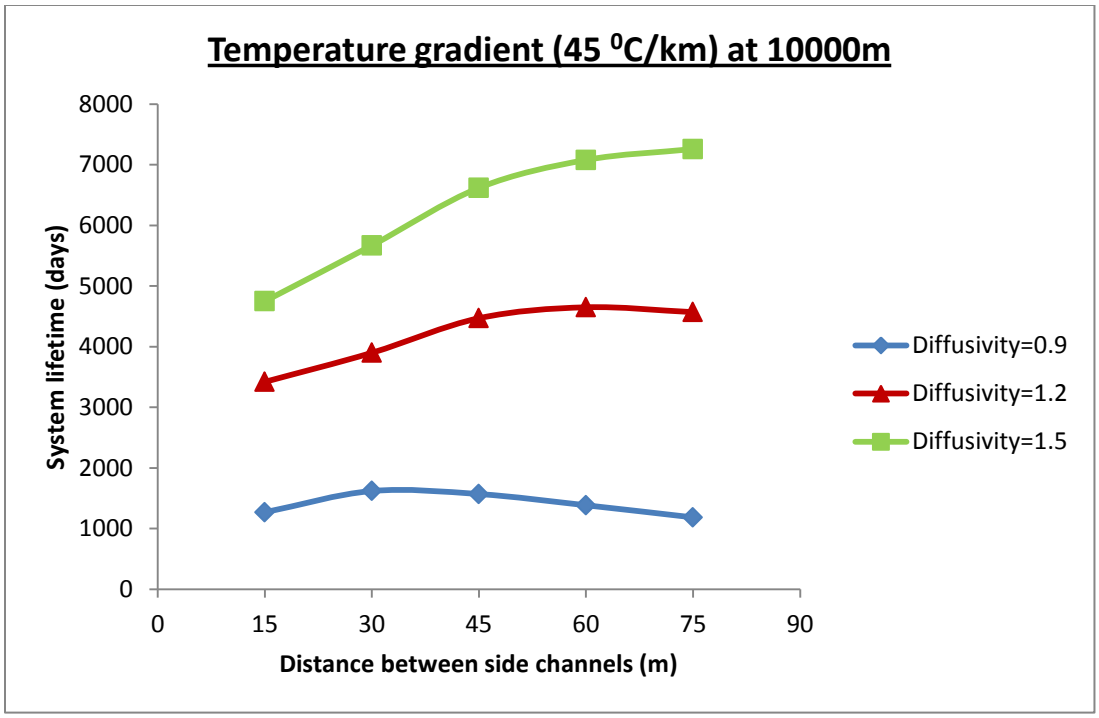

Figure5.3: System lifetime with respect to the distance between channels for a geothermal gradient of 45^{0}C/km and a total drilling length of 10000m.

The performance of the system at a temperature gradient of 45^{0}C/km and a total drilling length of 10,000m is shown in Figure 5.3. The target of 17-year system lifetime and 2 MW power generation is achieved only at a thermal diffusivity of 1.5 mm^2/s. The optimal distance between the side channels is around 75 m in this case.

The maximum lifetimes of the system at the other two thermal diffusivity values of 0.9 and 1.2 mm^2/s are respectively equal to 1570 and 4650 days, which are too short compared with the required target. Therefore, one can conclude that the system is not economically feasible for locations with a geothermal gradient of 45^{0}C/km at lower thermal diffusivity values of 0.9 and 1.2 mm^2/s.

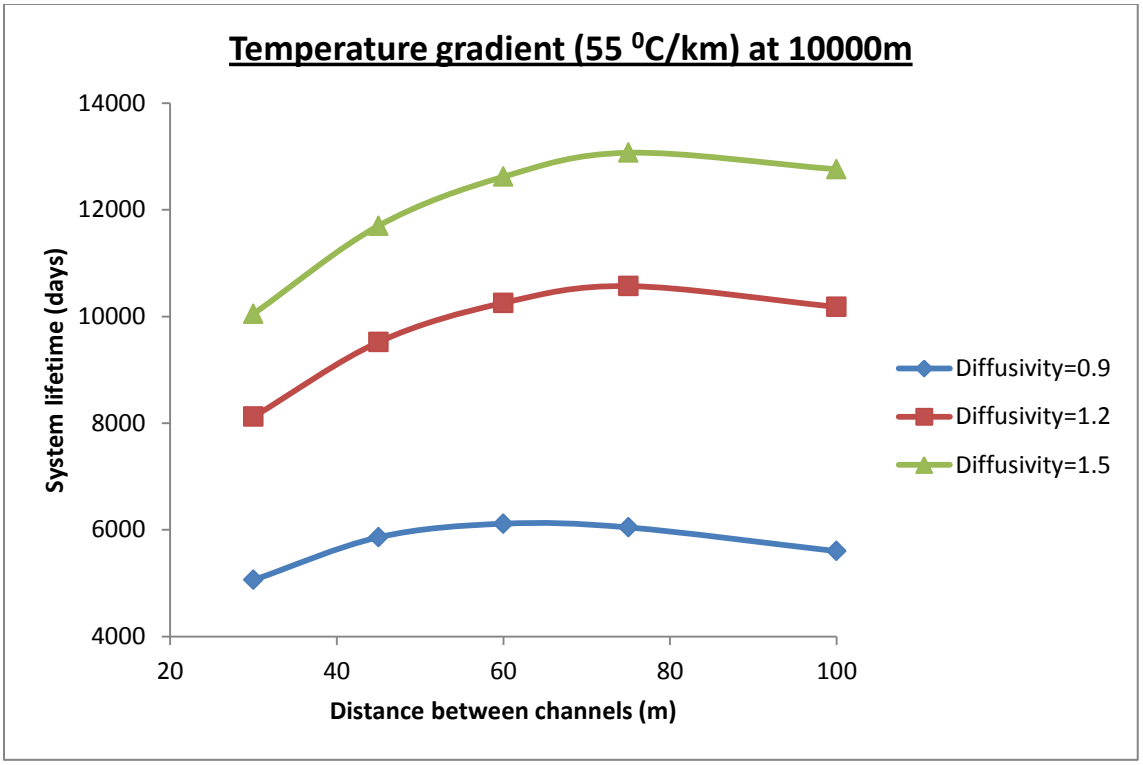

Figure5.4: System lifetime with respect to the distance between channels for a geothermal gradient of 55⁰C/km and a total drilling length of 10,000m

Figure 5.4 shows the performance of the system at a temperature gradient of 55⁰C/km and a total drilling length of 10,000m. The system lifetime in this condition has achieved the target of a 17-year system lifetime and 2 MW power generation at thermal diffusivity values of 1.2 mm²/s and 1.5 mm²/s. At a thermal diffusivity of 0.9 mm²/s, the maximum system lifetime is equal to 2,800 days which is too short compared to the required target. The optimal distance between side channels was found to be 75 m for both thermal diffusivity values of 1.2 mm²/s and 1.5 mm²/s. Therefore, one can conclude that

the system is economically feasible for locations with a geothermal gradient of 55^0C/km at thermal diffusivity values of 1.2 mm^2/s and higher, while is not feasible for a thermal diffusivity of 0.9 mm^2/s.

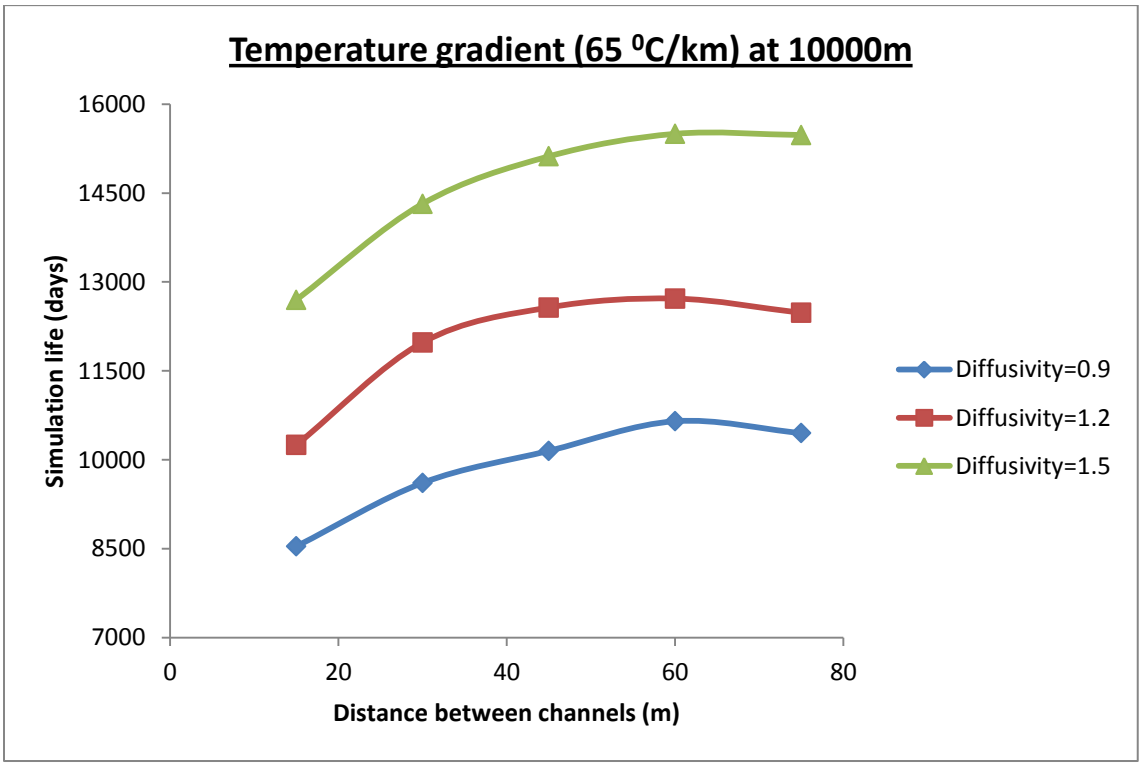

Figure5.5: System lifetime with respect to the distance between channels for a geothermal gradient of 65^0C/km and a total drilling length of 10,000m

The performance of the system at a temperature gradient of 65 ^{0}C/km and a total drilling length of 10,000 m is shown in Figure 5.5. The target of 2 MW power generation and a 17-year system lifetime has been achieved at different thermal diffusivity values of

0.9, 1.2, and 1.5 mm^2/s. The maximum system lifetime is equal to 15,500 days, which is exceedingly high compared to the target, and was obtained at a thermal diffusivity of 1.5 mm^2/s, as expected. The optimal distance between side channels was found to be 60 m in all cases. Therefore, one can state that the system is economically feasible for locations with a geothermal gradient of $65^0C/km$ and thermal diffusivity values of 0.9 mm^2/s and higher.

5.3.2. Total drilling length of 8,000 m

The next analysis is of the performance of the system at a total drilling length of 8,000m by considering similar values for thermal diffusivity and geothermal gradient.

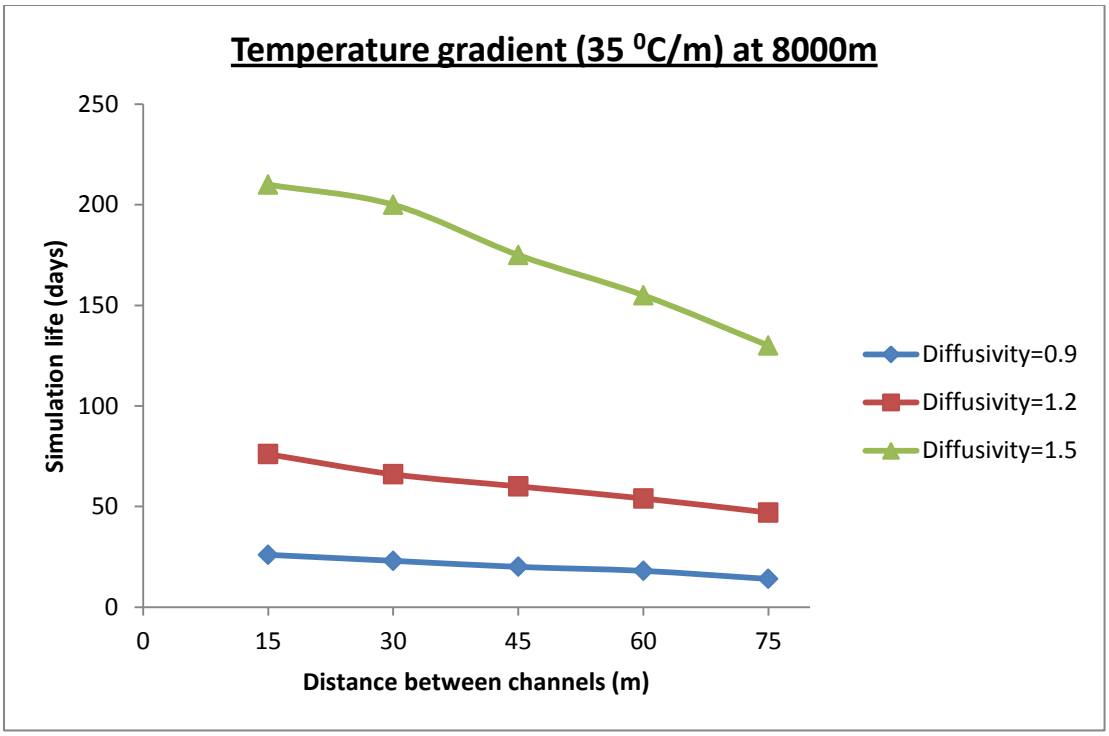

Figure5.6: System lifetime with respect to the distance between channels for a geothermal gradient of 35^{0}C/km and a total drilling length of 8,000m

The performance of the system at a temperature gradient of 35^{0}C/km and a total drilling length of 8,000m is shown in Figure 5.6. It can observed that the lifetime of the system is very short compared to the required target of 2 MW power generation and a 12-year system lifetime. The maximum system lifetime is equal to 210 days, which was obtained at a thermal diffusivity of 1.5 mm^2/s, and the optimal distance between side channels is 15 m. However, this does not achieve the target of a 12-year system lifetime as obtained from the economic analysis. Thus, one can conclude that the system is not economically feasible for locations with a thermal gradient of 35^{0}C/km.

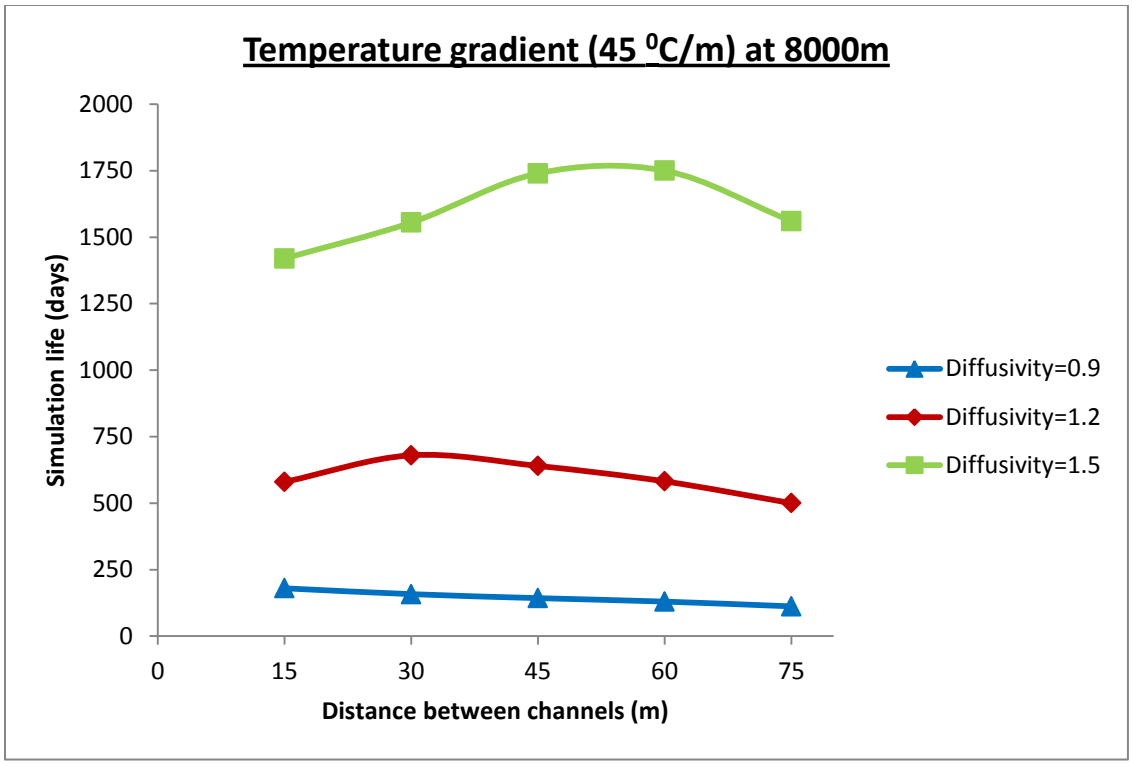

Figure5.7: System lifetime with respect to the distance between channels for a geothermal gradient of 45^{0}C/km and a total drilling length of 8000m

The performance of the system at a temperature gradient of 45^{0}C/km and a total drilling length of 8,000m is shown in Figure 5.7. The system lifetime is very short and does not achieve the required target of 2 MW power generation and a 12-year system lifetime at thermal diffusivity values of 0.9, 1.2, or 1.5 mm^2/s. The maximum system lifetime of 1,750 days was obtained at a thermal diffusivity value of 1.5 mm^2/s. The optimal distance between side channels is 45 m. However, these values do not achieve the required target, and hence one can state that the system is not economically feasible for locations with a geothermal gradient of 45^{0}C/km.

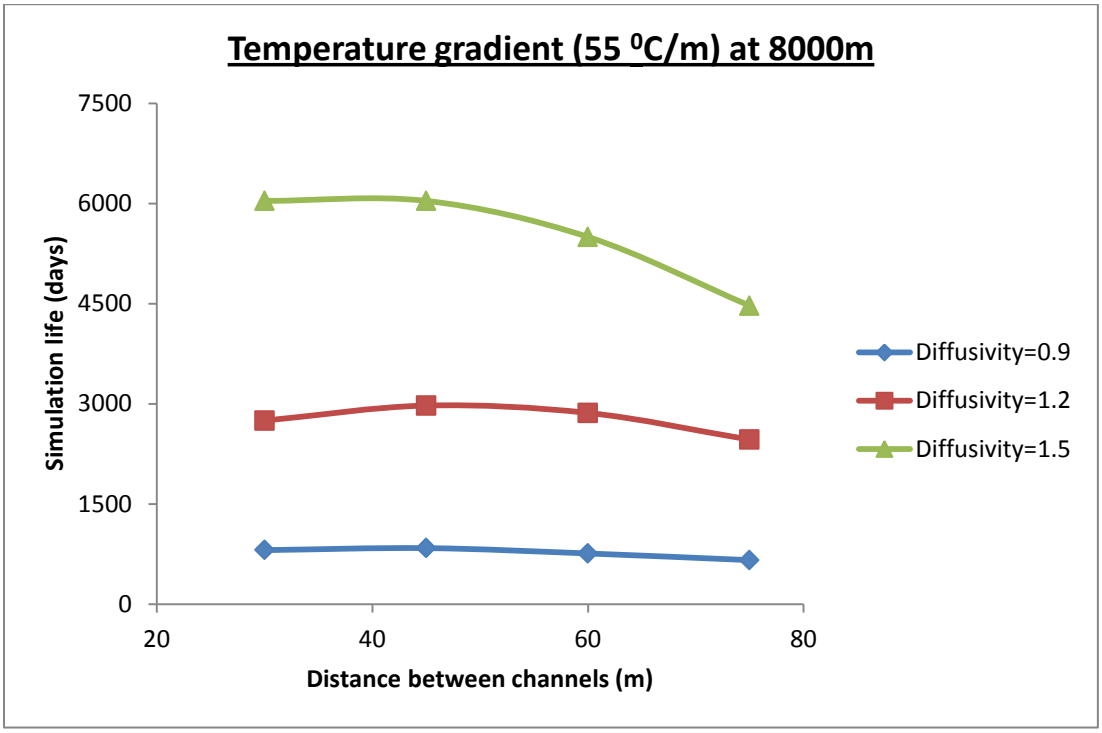

Figure5.8: System lifetime with respect to the distance between channels for a geothermal gradient of 55^{0}C/km and a total drilling length of 8,000m

The performance of the system at a temperature gradient of 55^{0}C/km and a total drilling length of 8,000m is shown in Figure 5.8. The required target of a 12-year system lifetime and 2 MW power generation is achieved only at a higher thermal diffusivity value of 1.5 mm^2/s. The maximum system lifetimes for the other thermal diffusivity values of 0.9 and 1.2 mm^2/s are 840 days and 2,900 days respectively, which are too short when compared to the required target. The optimal distance between side channels is found to be 45 m. Therefore, one can state that the system is economically feasible for locations with a geothermal gradient of 55^{0}C/km and thermal diffusivity of 1.5 mm^2/s.

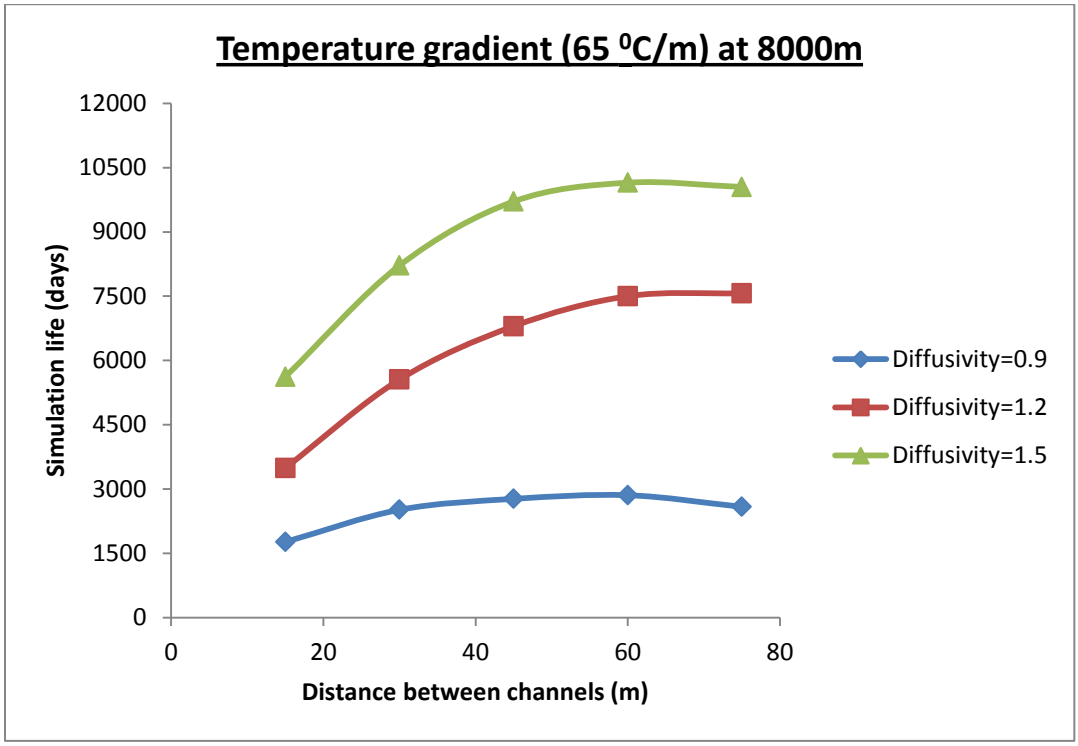

Figure5.9: System lifetime with respect to the distance between channels for a geothermal gradient of 65⁰C/km and a total drilling length of 8,000m

The performance of the system at a temperature gradient of 65 ^{0}C/km and a total drilling length of 8,000m is shown in Figure 5.9. The required target of 2 MW power generation and a 12-year system lifetime is achieved at higher thermal diffusivity values of 1.2 mm^2/s and 1.5 mm^2/s. The maximum system lifetime obtained for a thermal diffusivity of 0.9 mm^2/s is 2,800 days which is very short when compared to the required target. The optimal distance between side channels is found to be 60 m. Therefore, one can conclude that the system is economically feasible for locations with a geothermal gradient of 65C/km and thermal diffusivity of 1.2 or 1.5 mm^2/s.

To conclude this chapter, the optimal design parameters and the corresponding system lifetime for various geothermal gradients and thermal diffusivity values for deep geothermal drilling depths of 8,000 and 10,000 m were obtained. Also, the economic feasibility of the system under various conditions is discussed. A summary of the numerical results is presented in the next chapter.

Chapter 6: Summary and Conclusions

Geothermal power plants are considered to be renewable energy sources. Deep geothermal systems help in generating electricity in an effective way which provides clean energy. Slowly and steadily, many countries around the world have started using geothermal power plant systems to provide electricity. Keeping the growing population in mind, the major aim of such systems is to provide people with the basic required energy.

The present study deals with deep geothermal systems with total drilling lengths of 8,000 m and 10,000 m. In this research, a number of simulations have performed analysing the cost with respect to the system requirements and maintaining the requirements, such as following the demand curve so that one does not compromise on the output power generated and the system lifetime. Also, the system design under varying conditions in order to test the system capacity and efficiency has been analysed.

Based on the results obtained in the present research, a number of conclusions were drawn. The system lifetime depends on the depth of the main well; i.e. as the depth of the main well increases, the lifetime of the system is increased, as expected. This dependence

was quantified in Chapter 5. Moreover, as the geothermal gradient increases, the output power is increased, also as expected. Again, this relationship was quantified in Chapter 5.

Based on the depth of the main well, the length and number of side channels had an impact. The optimal distance between the side channels was found to be between 60 m and 75 m. Closer than this leads to an interaction between the side channels, and farther leads to having side channels in shallower depths, resulting in less power production. The number of side channels was determined based on optimal power generation.

The total drilling length of the system was kept to be 10,000m or 8,000m, since the focus of the present study is on deep geothermal systems. The results with thermal diffusivities of 1.2 and 0.9 mm^2/s do not seem to be as convincing as with a thermal diffusivity of 1.5 mm^2/s. Also, the results in certain cases with low thermal diffusivity or low thermal gradient do not satisfy the demand curve requirements for the 12-year (for the 8,000 m depth) or 17-year (for the 10,000 m depth) lifetime requirement of the systems.

For example, for the case of 10,000 m total drilling length and a geothermal gradient of $55^0C/km$, the best optimal design parameters are presented in Table 6.1.

Table6.1: Optimal design conditions for geothermal gradient of 55^{0}C/Km

Total drilling length	**10000 (m)**
Total lifetime of the system	35 years
Thermal diffusivity	1.5 mm2/s
Length of channel	106.25 m
Length of main well	5,000 m
Vertical distance between channels	75 m
Angle	40 degrees

The sustainable lifetimes of 2 MW single-well deep geothermal energy systems are presented in Tables 6.2 to 6.5 for a practical range of geophysical parameters. As can be observed in those tables, deep geothermal energy systems can be used to generate 2 MW of energy for more than 17 years, depending on the thermal diffusivity and geothermal gradient. Moreover, the optimal conditions of the system for a total drilling length of 8,000m and 10,000m are presented in those tables under various geothermal gradients and thermal diffusivities. All these conditions are analysed based on the feasibility of the system with respect to the financial analysis. The shaded portions in the Tables 6.2 to 6.5 show the cases where the system is not economically feasible, and the non-shaded portions show the economically feasible cases.

Table6.2: Optimal conditions and system lifetime for geothermal gradient of 35^0C/km (shaded region shows the economically unfeasible area)

Total drilling length of the system	Thermal diffusivity 0.9 mm^2/s		Thermal diffusivity 1.2 mm^2/s		Thermal diffusivity 1.5 mm^2/s	
	Optimal distance (m)	System lifetime (days)	Optimal distance (m)	System lifetime (days)	Optimal distance (m)	System lifetime (days)
8,000m	15	26	15	76	15	210
10,000m	15	171	30	700	45	1,800

Table6.3: Optimal conditions and system lifetime for geothermal gradient of 45^0C/km (shaded region shows the economically unfeasible area)

Total drilling length of the system	Thermal diffusivity 0.9 mm^2/s		Thermal diffusivity 1.2 mm^2/s		Thermal diffusivity 1.5 mm^2/s	
	Optimal distance (m)	System lifetime (days)	Optimal distance (m)	System lifetime (days)	Optimal distance (m)	System lifetime (days)
8,000m	15	180	30	680	60	1,750
10,000m	30	1,620	60	4,650	75	7,260

Table6.4: Optimal conditions and system lifetime for geothermal gradient of 55^0C/km (shaded region shows the economically unfeasible area)

Total drilling length of the system	Thermal diffusivity 0.9 mm^2/s		Thermal diffusivity 1.2 mm^2/s		Thermal diffusivity 1.5 mm^2/s	
	Optimal distance (m)	System lifetime (days)	Optimal distance (m)	System lifetime (days)	Optimal distance (m)	System lifetime (days)
8,000m	45	840	45	2,975	30-45	6,040
10,000m	60	6,115	75	10,570	75	13,070

Table6.5: Optimal conditions and system lifetime for geothermal gradient of 65^0C/km (shaded region shows the economically unfeasible area)

Total drilling length of the system	Thermal diffusivity 0.9 mm^2/s		Thermal diffusivity 1.2 mm^2/s		Thermal diffusivity 1.5 mm^2/s	
	Optimal distance (m)	System lifetime (days)	Optimal distance (m)	System lifetime (days)	Optimal distance (m)	System lifetime (days)
8,000m	60	2855	60	7,500	60	10,150
10,000m	60	10,650	60	12,720	60	15,500

Finally, the optimal lifetime of the system with respect to thermal diffusivity for total drilling lengths of 8,000m and 10,000 m for various geothermal gradients are summarized in Figures 6.1 and 6.2, where again the shaded region shows the economically unfeasible cases.

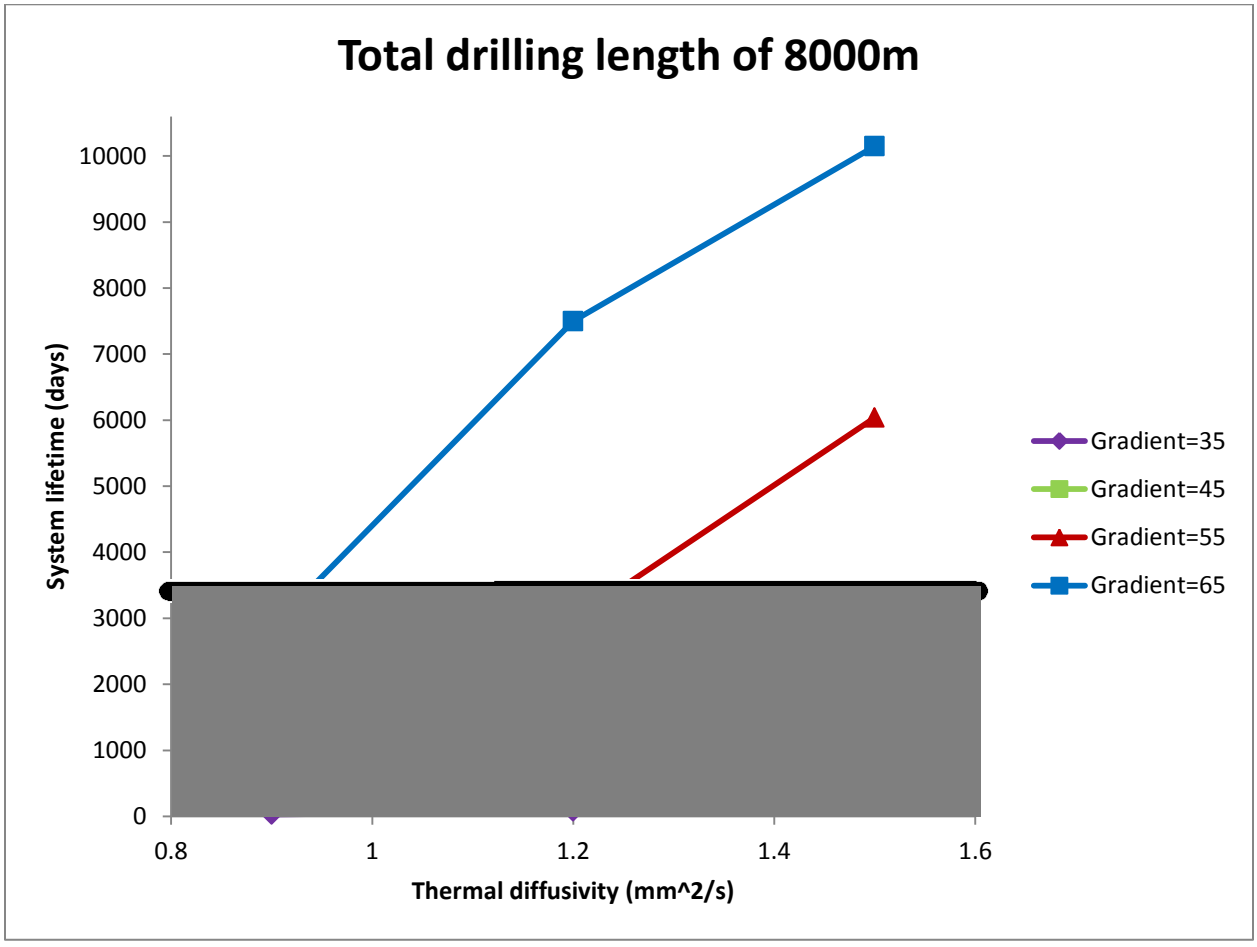

Figure6.1: Optimal lifetime with respect to thermal diffusivity for total drilling length of 8,000m for various geothermal gradients (shaded region shows the economically unfeasible area)

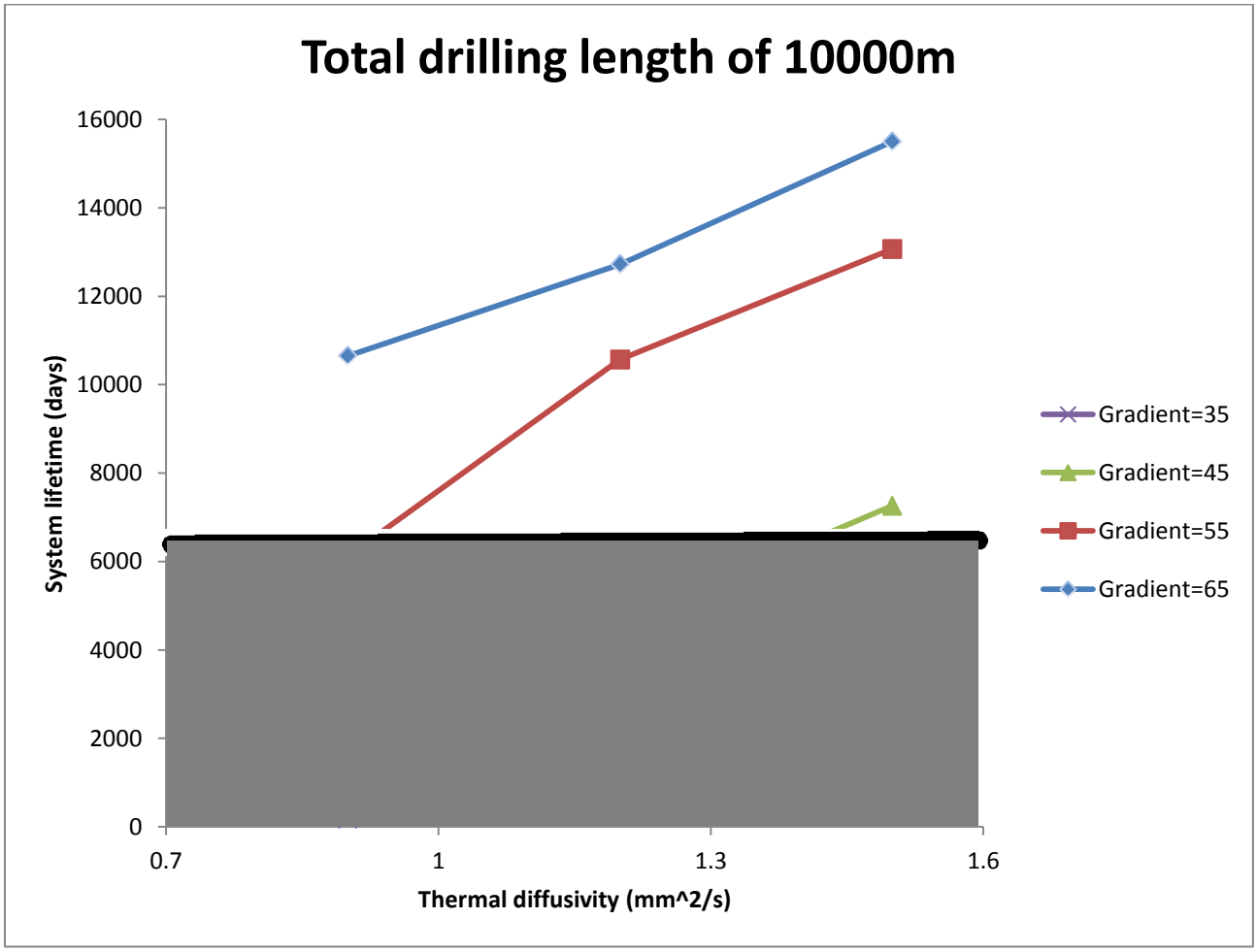

Figure6.2: Optimal lifetime with respect to thermal diffusivity for total drilling length of 10,000m for various geothermal gradients (shaded region shows the economically unfeasible area)

Future studies:

Based on the results and conclusion, the following issues are suggested for the future studies:

- Finding the performance of the system at lower thermal gradients.
- Changing the depth of the main well based on the total drilling length of the system and check its performance.
- Evaluating different ways to decrease the initial cost which will give returns faster.
- Improving the system design and finding ways of generating more thermal energy.

7. References

1) Heidinger, 2009. Integral modelling and financial impact of the geothermal situation and power plant at Soultz-sous- Forets, France.
2) Kaygusuz and Kaygusuz, 2004. Geothermal energy in Turkey: The sustainable future.
3) Stefansson, 1996. Geothermal reinjection experience, Orkustofnun, National energy authority, Grensdsvegur 9, IS-108 Reykjavik, Iceland.
4) N. Cuenot, EEIG "Heat Mining", J-P. Faucher, EEIG "Heat Mining", D. Fritsch, EEIG "Heat Mining", A. Genter, EEIG "Heat Mining", and D. Szablinski, Pfalzwerke AG, 2005. The European EGS project at Soultz-sous-Forets: from extensive exploration to power production.
5) Parrella; Micheal J., 2010. System and method of maximizing heat transfer at the bottom of a well using heat conductive components and a predictive model.
6) Tolis and Rentizelas, 2011. An impact assessment of electricity and emission allowances pricing in optimised expansion planning of power sector portfolios, applied energy.
7) http://www.doran-ge.ie/geothermaldrilling.html
8) Rummel F, 1990. Physical Properties of the rock in the granitic section of borehole GPK1, Soultz-Sous-Forets, Report BMFT 26579 A+B /EC EN-3G-0092-D, Institute of Geophysik, Ruhr University, Bochum, Germany.
9) http://encyclopedia2.thefreedictionary.com/Heat-pipe

10) http://www.energysavers.gov/your_home/space_heating_cooling/index.cfm/mytopic=12650

11) Milora and Tester, 1976. Geothermal heat as a source of electric power. The Massachusetts Institute of technology press, Cambridge, Massachusetts, 195pp.

12) Dr. Hadi Saadat, 2010. Power system analysis third edition for the analysis of power systems using software.

13) http://geothermal.marin.org/geopresentation/sld049.htm

14) Ozean and Gokeen, 2010. Performance Analysis of Single – Flash Geothermal Power Plants: Gas removal systems point of view, Mechanical Engineering department, Izmir University of Technology, Urla, and Izmir, Turkey.

15) http://geothermal.marin.org/geopresentation/sld054.htm

16) Yamada and Oyama. Small Capacity geothermal binary power generation systems. Japan.

17) http://geothermal.marin.org/geopresentation/sld059.htm

18) Goldstein et al. 1999. Heat transfer- a review of 1999 literature, Heat and mass transfer.

19) Haas et al., 2010. A historical review of promotion strategies for electricity from renewable energy sources in EU countries; Renewable and sustainable energy reviews.

20) Heuer. N., 1988. Modelling the geines of HDR-systems, Diplomarbeit. Institute of Mathematics, University of Hannover, 67pp.

21) World Oil, 2004. Drill bit designs evolve to handle new challenges, Defining technology for exploration, drilling and production.

22) Moss et al., 2002. Directional technology, steerable systems advance. Drilling contractor.

23) Quasching, 2010. 10 Geothermal energy- Power from the deep, Renewable energy and climate change.

24) Garnish, 1987, Legarth and Wohlgemuth, 2003. HDR economic modelling: HDRec software, Volume 35, Issues 5-6, October-December 2006, Pages 683-710.

25) Diersch et al. 2010. Finite element model for borehole heat exchanger (BHE) systems.

26) Ou and Einav, 2010. Simplified model: Fluid temperature and power estimation of geothermal power plants.

27) Mottaghy and Dijkshoorn, 2012. Implementation of an effective finite difference model for borehole heat exchangers using heat and mass transport equations.

28) Lazzari et al. 2010. Long term performance of BHE fields with negligible groundwater movement.

29) Ozgener and Hepbasli, 2005. Modeling and performance evaluation of ground source (geothermal) heat pumps systems: Energetic modeling of ground source heat pump (GSHP)

30) Bauer et al. 2010. Development and application of a transient three dimensional (3D) analysis of borehole heat exchanger modeling.

31) Teza et al. 2010. Analysis of long term irregular shaped borehole heat exchanger system with real pattern and regular grid approximation.

32) Valladares et al. 2005. Numerical modeling of flow processes inside geothermal wells: An approach for prediction production characteristics with uncertainties.

33) Paly et al. 2012. Optimization of energy extraction for closed shallow geothermal systems using linear programming.

34) Meer et al. 2008. Time dependent shape functions for modeling highly transient conductive heat flow in geothermal systems.

35) Zeng et al. 2003. Heat transfer analysis of boreholes in vertical ground heat exchangers.

36) Yang et al. 2009. Review of models and systems of the vertical borehole ground coupled heat pumps.

37) Lamarche and Beauchamp, 2006. A new contribution to the finite line source model for geothermal boreholes.

38) Lim et al. 2006. An experimental study on the thermal performance of ground heat exchanger.

39) Florides et al. 2011. The analysis of heat flow through a borehole heat exchanger validated model.

40) Eslami-nejad and Bernier, 2011. The coupling of geothermal heat pumps with thermal solar collectors using double U tube boreholes with two independent circuits.

41) Mendez et al. 2010. Evaluation of MT3DMS for heat transport simulation of closed geothermal systems.

42) Li et al. 2006. The simulation and experiment on the thermal performance of U-vertical ground coupled heat exchanger.

43) Choi et al. 2011. Numerical simulation of vertical ground heat exchangers for unsaturated soil conditions.

Appendix I

I.1 System lifetime with respect to distance between side channels

In this appendix, the numerical results for the system lifetime with respect to distance between side channels for various total drilling lengths and geothermal gradients are presented. The shaded portions represent the economically unfeasible cases whereas the non-shaded portions correspond to the feasible cases.

Table I.1: System lifetime with respect to distance between side channels for total drilling length of 10000(m) and geothermal gradient of 35^0C/km (shaded region shows the economically unfeasible area)

Distance between side channels (m)	Life time of the system		
	Thermal diffusivity 0.9 mm^2/s	Thermal diffusivity 1.2 mm^2/s	Thermal diffusivity 1.5 mm^2/s
15m	171	628	1215
30m	150	700	1710
45m	125	610	1800
60m	110	500	1690
75m	95	430	1480

Table I.2: System lifetime with respect to distance between side channels for total drilling length of 8000(m) and geothermal gradient of 35^0C/km (shaded region shows the economically unfeasible area)

Distance between side channels (m)	Life time of the system		
	Thermal diffusivity 0.9 mm^2/s	Thermal diffusivity 1.2 mm^2/s	Thermal diffusivity 1.5 mm^2/s
15m	26	76	210
30m	23	66	200
45m	20	60	175
60m	18	54	155
75m	14	47	130

Table I.3: System lifetime with respect to distance between side channels for total drilling length of 10000(m) and geothermal gradient of 45^0C/km (shaded region shows the economically unfeasible area)

Distance between side channels (m)	Life time of the system		
	Thermal diffusivity 0.9 mm^2/s	Thermal diffusivity 1.2 mm^2/s	Thermal diffusivity 1.5 mm^2/s
15m	1270	3420	4750
30m	1620	3900	5670
45m	1570	4470	6620
60m	1380	4650	7080
75m	1185	4570	7260

Table I.4: System lifetime with respect to distance between side channels for total drilling length of 8000(m) and geothermal gradient of 45^{0}C/km (shaded region shows the economically unfeasible area)

Distance between side channels (m)	Life time of the system		
	Thermal diffusivity 0.9 mm^2/s	Thermal diffusivity 1.2 mm^2/s	Thermal diffusivity 1.5 mm^2/s
15m	180	580	1420
30m	158	680	1555
45m	143	640	1740
60m	130	582	1750
75m	112	500	1560

Table I.5: System lifetime with respect to distance between side channels for total drilling length of 10000(m) and geothermal gradient of 55^{0}C/km (shaded region shows the economically unfeasible area)

Distance between side channels (m)	Life time of the system		
	Thermal diffusivity 0.9 mm^2/s	Thermal diffusivity 1.2 mm^2/s	Thermal diffusivity 1.5 mm^2/s
30m	5060	8120	10050
45m	5860	9520	11700
60m	6115	10255	12620
75m	6045	10570	13070
100m	5600	10180	12760

Table I.6: System lifetime with respect to distance between side channels for total drilling length of 8000(m) and geothermal gradient of 55^0C/km (shaded region shows the economically unfeasible area)

Distance between side channels (m)	Life time of the system		
	Thermal diffusivity 0.9 mm^2/s	Thermal diffusivity 1.2 mm^2/s	Thermal diffusivity 1.5 mm^2/s
30m	810	2750	6040
45m	840	2975	6040
60m	760	2865	5500
75m	660	2465	4470

Table I.7: System lifetime with respect to distance between side channels for total drilling length of 10000(m) and geothermal gradient of 65^0C/km (shaded region shows the economically unfeasible area)

Distance between side channels (m)	Life time of the system		
	Thermal diffusivity 0.9 mm^2/s	Thermal diffusivity 1.2 mm^2/s	Thermal diffusivity 1.5 mm^2/s
15m	8540	10250	12700
30m	9610	11980	14320
45m	10150	12570	15120
60m	10650	12720	1550
75m	10450	12480	15480

Table I.8: System lifetime with respect to distance between side channels for total drilling length of 8000(m) and geothermal gradient of 65^{0}C/km (shaded region shows the economically unfeasible area)

Distance between side channels (m)	Life time of the system		
	Thermal diffusivity 0.9 mm^2/s	Thermal diffusivity 1.2 mm^2/s	Thermal diffusivity 1.5 mm^2/s
15m	1765	3490	5620
30m	2515	5555	8215
45m	2770	6800	9710
60m	2855	7500	10150
75m	2585	7570	10050

Appendix II

II.1 Present value (P) analysis:

In this Appendix, sample calculations for present value analysis are presented. A typical case with total drilling length 10000m is considered. The present value is calculated for the case of total lifetime equal to 25 years. The total capital in this case is $ 4,300,000.

The time period considered for the investment = 25 years (i.e., 300 months)

The interest rate (i) = 0.5 % per month.

But, to achieve a more realistic figure one needs to consider the inflation rate considering the inflation effect in the real world.

Inflation rate (f) = 0.0013 per month.

The real interest (i) =

$$i_{real} = \frac{i - f}{1 + f}$$

i_{real}= (0.005-0.0013)/(1+0.0013)

= 0.0037 / month

One can calculate the present value as follows:

$$P = F\frac{\left[(1+i)^n - 1\right]}{i(1+i)^n}$$

Therefore, noting that the initial cost is $4300000, monthly electricity income is $36720 and monthly maintenance is $5500, the total present value can be calculated as

P= -4300000+ (36720-5500)*[(1+0.0037)^{300}-1/ 0.0037*(1+0.0037)^{300}]

=-4300000+ [(31220)*(181.071)]

=-4300000+5653005

=**1,353,005 (1.3 Million)**

Therefore, the estimated present value for this system for a lifetime of 25 years is $**1.3M.**